geosciences

MDPI

Article

Vegetation, Climate and Habitability in the Marseille Basin (SE France) *circa* 1 Ma

Valérie Andrieu [1,*], Pierre Rochette [1], François Fournier [1], François Demory [1], Mary Robles [1], Odile Peyron [2], Séverine Fauquette [2], Eliane Charrat [3], Pierre Magniez [4], Belinda Gambin [5] and Samuel Benoît De Coignac [1]

1 Aix-Marseille University, CNRS, IRD, INRAE, CEREGE, 13545 Aix-en-Provence, France; rochette@cerege.fr (P.R.); fournier@cerege.fr (F.F.); demory@cerege.fr (F.D.); robles@cerege.fr (M.R.); samuel.benoit-de-coignac@developpement-durable.gouv.fr (S.B.D.C.)
2 Université de Montpellier, CNRS, IRD, 34090 Montpellier, France; odile.peyron@umontpellier.fr (O.P.); severine.fauquette@umontpellier.fr (S.F.)
3 Aix-Marseille University, CNRS, IRD, 13545 Aix-en-Provence, France; eliane.charrat@imbe.fr
4 Aix Marseille University (AMU), CNRS, Minist. Culture, INRAP, LAMPEA, 13090 Aix-en-Provence, France; pierre.magniez@univ-amu.fr
5 Institute of Earth Systems, University of Malta, MSD 2080 Msida, Malta; belinda.gambin@um.edu.mt
* Correspondence: andrieu@cerege.fr

Abstract: The environment of the Marseille basin in the Early Pleistocene was reconstructed through a multiproxy study of fluvial tufa deposits. Palaeomagnetic measurements revealed the Jaramillo subchron and dated the tufa to within the 0.8–1.5 Ma interval, probably between 0.9 and1.2 Ma. Sedimentological studies show varied depositional environments comprising natural dams formed by accumulations of plants promoting the development of upstream water bodies. The very negative $\delta^{13}C$ values indicate that the Marseille tufa is not travertine *sensu stricto* but tufa deposited by local cold-water rivers. Palynological analyses indicate a semi-forested, diverse, mosaic vegetation landscape dominated by a Mediterranean pine and oak forest. Along the streams, the riparian forest was diverse and included *Juglans*, *Castanea*, *Platanus* and *Vitis*. The potential diet reconstructed from pollen was varied. The most surprising discovery was the presence of proto-cereals, which could potentially enrich the diet with carbohydrates. The identification of spores of coprophilous fungi seems to indicate the presence in situ of large herbivore herds. It is possible that, as in Anatolia, the disturbance of ecosystems by large herbivores was responsible for the genetic mutation of Poaceae and the appearance of proto-cereals. Climatic reconstructions indicate a slightly cooler and wetter climate than the present.

Keywords: Marseille France; Early Pleistocene; vegetation; potential diet; cereals; climate; depositional environment

check for updates

Citation: Andrieu, V.; Rochette, P.; Fournier, F.; Demory, F.; Robles, M.; Peyron, O.; Fauquette, S.; Charrat, E.; Magniez, P.; Gambin, B.; et al. Vegetation, Climate and Habitability in the Marseille Basin (SE France) *circa* 1 Ma. *Geosciences* **2024**, *14*, 211. https://doi.org/10.3390/geosciences14080211

Academic Editors: Marta Bąk, Dangpeng Xi and Erik Wolfgring

Received: 31 May 2024
Revised: 23 July 2024
Accepted: 24 July 2024
Published: 7 August 2024

Copyright: © 2024 by the authors. Licensee MDPI, Basel, Switzerland. This article is an open access article distributed under the terms and conditions of the Creative Commons Attribution (CC BY) license (https://creativecommons.org/licenses/by/4.0/).

1. Introduction

Tufa and travertine are freshwater carbonates along streams and in pools whose banks are ideal breeding grounds for a wide variety of plants and animals, including hominins, e.g., [1,2]. This was particularly the case at about 1.2 Ma in the Denizli travertine complex in SW Anatolia, which is related to hot water springs e.g., [3–5]. The Marseille calcareous tufa, formed in cool water streams and pools [6], lies at the other end of the Mediterranean Basin, on the route that herds of large herbivores and hominins may have followed in their migratory dynamics towards the Iberian Peninsula, where hominin fossils are found at 1.5 Ma in the Guadix–Baza–Orce basin [7,8] and at 1.1–1.2 Ma in Sima de Elefante, Atapuerca [9,10]. On the French Mediterranean coast, earlier traces of hominins can be found at the Vallonnet [11] and Bois de Riquet [12] sites. Between these two sites lies the Marseille basin, which may have been frequented by hominins and herds of large herbivores during the Pleistocene. The study of Pleistocene tufa, which extensively outcrops within the Marseille basin, has been neglected since early research [13]. The diversity of floristic

assemblages is underlined in the bibliography [14,15], but no new palaeontological data have been acquired since the end of the 19th century. The geological framework has been studied a little better [16,17]. In these studies, the Marseille tufa is considered to be a Pleistocene-age formation, with no further details. From an archaeological point of view, to our knowledge, there have been no discoveries of lithic material or other traces of hominin presence. However, the Marseille basin could have been a potential dwelling site during the westward migration of the first hominins.

Tufa and travertine are considered poor material for pollen preservation [18] due to the oxidising depositional conditions that preside over their emplacement. Post-depositional contamination by pollen may arise due to the porosity and permeability of these rock types. However, there exists indurated, non-porous facies where in situ pollen can be preserved, as is the case in the Denizli travertine and Marseille calcareous tufa. On the other hand, they can be rich in macrofossils, such as large mammal bones, vegetation remains (e.g., leaves, fruit, tree branches and trunks), or sometimes even plant imprints [4,19]. In the Marseille tufa, few animal macrofossils have been found—just a few fragments of a tusk and a tooth of the southern mammoth (*Mammuthus meridionalis*)—as well as several teeth of the straight-tusked elephant (*Palaeoloxodon antiquus*) [16], suggesting the latest Villafranchian period [20]. The revisit of the material still accessible in collections [16] (eight teeth among the twelve cited) confirmed and modernised the identification of two Pleistocene species: *Mammuthus meridionalis* and *Palaeoxodon* (previously *Elephas*) *antiquus* [21]. The first species is the most represented and the only one with a well-documented localisation within the travertine of La Viste. Both species correspond to the assemblage arriving around 0.8–1.2 Ma in Southern Europe [22]. *Palaeoxodon antiquus* points toward the younger part of this time window.

The study of plant macro-remains [13,23] yielded more abundant results, with the identification of 32 plant taxa, 10 of which are shared at the genus level with the pollen taxa published in this article and 15 of which are present only as macro-remains (Table 1). These taxa include plants found today in the laurel forests of the Macaronesian islands (e.g., *Laurus canariensis*, *Phoebe barbusana*) or in the thermo-Mediterranean zone (e.g., *Pinus salzmannii*, *Chamaerops humilis*, *Magnolia vasseuri* and *Nerium oleander*). The identification of *Laurus canariensis* [13] is questioned and attributed to *Laurus nobilis* [23]. The malacofauna of the tufa indicates an open, xerothermic Mediterranean environment, close to the current malacological associations of the Marseille coastline, with the presence of *Cernuella virgata* Da Costa, *Trochoidea trochoides* Poiret and *Candidula unifasciata* Poiret [24]. The advantage of plant and animal macro-remains is that they can be identified at a more precise taxonomic level than pollen. They also testify to their in situ origin or, in the case of transport by the watercourses that flowed over the tufa, to their local origin, based on the fact that the watershed of the tufa studied sites is of the order of less than 10 km and the poor preservation of macro-remains during transport. Pollen, on the other hand, reveal a greater taxonomic diversity of plants and enable us to reconstruct the biodiversity of ecosystems, plant landscapes and climate on a regional and local scale.

In this article, we present the results of (1) palaeomagnetic measurements, which provides age constraints for the tufa; (2) sedimentological analyses, which allow us to reconstruct the depositional environment of the tufa; (3) pollen analyses and related climatic reconstructions that enable us to reconstruct plant landscapes, the potential diet available to hominins and the climates that existed at the time the tufa was laid down.

Table 1. List of plants (pollen and NPP•, macro-remains*#) and NPPs identified in the Marseille tufa (this article, * [13], # [23]).

•*Abies* sp.	#Chamaerops humilis	#*Laurus nobilis*	•*Potentilla* sp.
**Acer monspessulanum*	•Charcoal	•*Ligustrum* sp.	•*Prunus* t.
•*Acer* sp.	•Chenopodiaceae	•*Lycopodium selago*	•*Quercus* (deciduous)
•*Alnus glutinosa* t.	•Chrysophyceae	**#Magniolia vasseuri*	#•*Quercus ilex*
•*Alnus viridis* sp.	•Cichorioideae	•*Malva* sp.	**Quercus pubescens*
•*Ammi* sp.	•*Cirsium* t.	**Malus acerba*	•*Reseda* sp.
•*Anthemis* sp.	**Cornus sanguinea*	•*Mentha* sp.	#*Ribes* sp.
•Apiaceae	**#Corylus avellana*	•Micro-foraminifera	**#Rubus idaeus*
•*Artemisia* sp.	•*Corylus* sp.	•*Myriophyllum spicatum*	•*Rumex* sp.
#*Arundo* sp.	**Crataegus oxycantha*	#*Nerium oleander*	•*Salix* sp.
•*Aster* t.	•Cyperaceae	•*Odontites* sp.	**Salix viminalis*
•*Atriplex* t.	•*Delitschia* sp.	•*Olea* sp.	•*Sambucus nigra*
•*Betula* sp.	•*Dipsacus* sp.	•*Ostrya/Carpinus orientalis*	#*Scolopendrium officinale*
•*Blackstonia* t.	•*Draba* t.	•*Pedicularis* t.	•*Secale cereale*
•*Botryococcus* sp.	•*Erica arborea/multiflora* t.	**Phoebe barbusana*	•*Sinapis* t.
*•*Buxus* sp.	•*Euphorbia* sp.	**Phragmites sp.*	#Sorbus domestica
•*Carduus* t.	•*Fagus* sp.	•*Picea* sp.	•*Sordaria* sp.
•*Castanea* sp.	**#Ficus carica*	#•*Pinus halepensis t.*	•*Tilia* sp.
•*Cedrus* sp.	•*Fraxinus* sp.	•*Pinus* (Mediterranean)	**#Tilia europaea*
**Celtis australis*	•*Galium* sp.	**Pinus nigra* subsp. *salzmannii*	#*Trachycarpus* t.
•*Celtis* sp.	•*Geranium* sp.	•*Pinus sylvestris*	•*Trifolium* t.
•*Centaurea cyanus* t.	•*Glomus* sp.	#*Pirus acerba*	•Type 200
•*Centaurea nigra* t.	•Gymnosperm micro-remains	•*Pistacia* sp.	•*Ulex* t.
**#Cercis siliquastrum*	•HdV20d	•*Plantago coronopus*	•*Ulmus* sp.
•Cerealia 40 µm	**Hedera helix*	•*Plantago lanceolata* t.	•*Urtica* sp.
•Cerealia 42.5 µm	•*Hypericum* sp.	•*Plantago major-media t.*	•*Valsaria* sp.
•Cerealia 45 µm	•*Iris* sp.	•*Platanus* sp.	•*Viburnum* sp.
•Cerealia 47.5 µm	•*Juglans* sp.	•Poaceae	**Viburnum tinus*
•Cerealia 52.5	•*Juniperus* sp.	**Populus alba*	#*Vitis vinifera* subsp. *sylvestris*
•Cerealia 55 µm	•Lamiaceae	#*Populus nigra*	•*Vitis* sp.
•Cerealia 60 µm	**Laurus canariensis*	•*Populus* sp.	

2. The Studied Sites and Sampling

The Marseille tufa deposit was formed during the Quaternary period, in the Oligocene basin of Marseille. It forms a discontinuous plateau, 10–20 m thick, situated between 50 and 170 m above sea level. It was deposited in a varied (fluvial, lacustrine, encrusting waterfalls) continental depositional environment. The main outcrops are to the NW and SE of the basin (Figure 1). When it was deposited, the tufa occupied the lowest points of the basin. It was dominated by hills of Oligocene siliclastic fluvial and lacustrine deposits [6]. Rivers flowing over the tufa flowed into the Mediterranean, whose coastline was situated a few kilometres south of the present-day location. Tectonic movements, global climatic changes and subsequent erosive dynamics are responsible for the present-day inversion of the relief, which explains the plateau position of the tufa today.

Three areas were sampled for the present study, four to the NW of the Marseille basin—La Viste (two sections), St Exupéry High School and La Calade—and three in the SE of the basin: Les Amaryllis, Les Olives quarry materials and Les Olives Avenue (Figure 1). A total of 23 large samples of about one cubic decimetre were taken at these seven sites (Figure 1, Supplementary File S1) for the pollen and petrographic analyses and were cut to get rid of the potential pollution from present-day pollen rain (Figure 2). All samples were obtained from the calcareous tufa formation, except a clay sample (Les Olives Avenue, Figure 1) that corresponds to the first layers below the tufa. The sites sampled correspond to former quarry faces or trenches dug for urbanisation purposes.

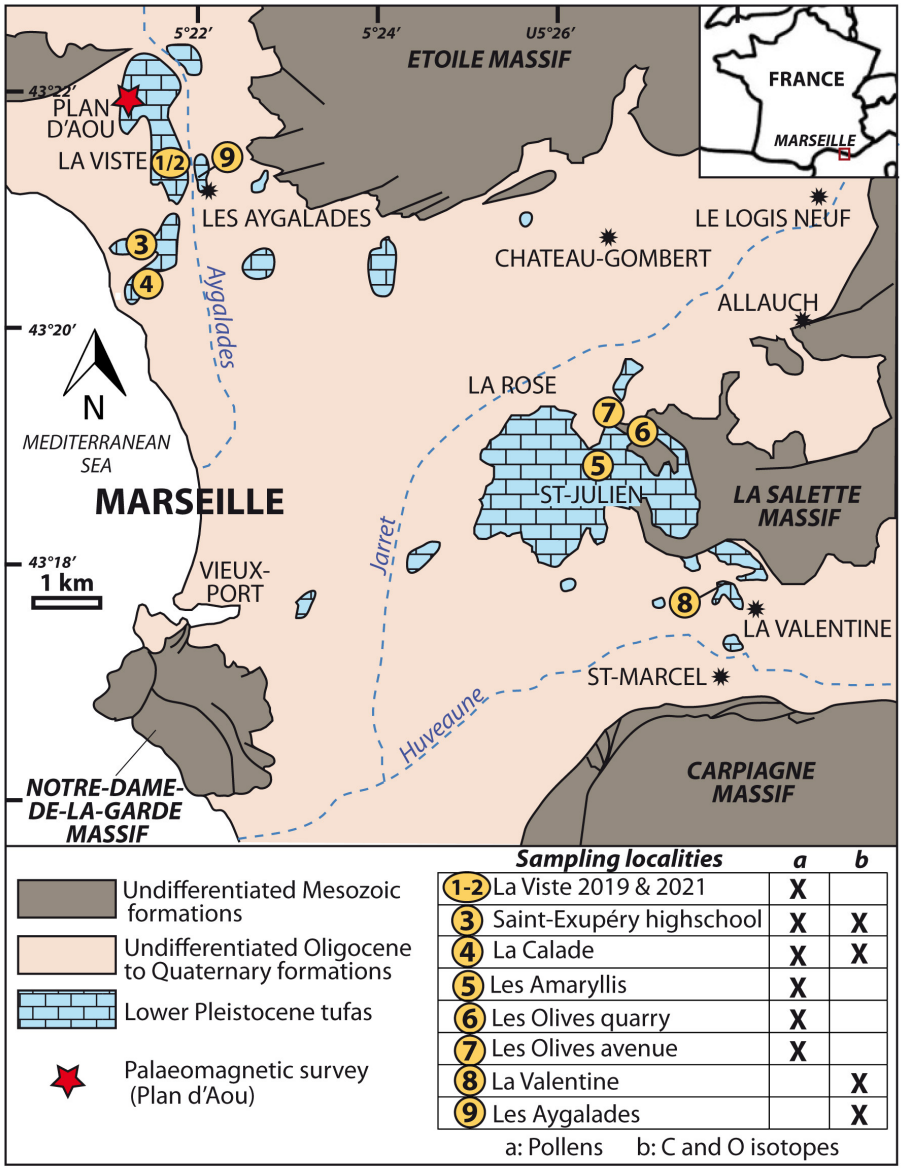

Figure 1. Simplified geological map of the Marseille basin and location of the samples.

To obtain palaeomagnetic dating constraints, oriented samples from three sites (La Viste, Saint-Exupéry High School and La Calade; Figure 1) that revealed significant pollen content were successively obtained using a portable drilling machine and orienting tools. Moreover, twenty-five years ago we independently sampled a nearby full section of the tufa with a circa 0.2 m interval at Plan d'Aou (La Viste) for palaeomagnetic purposes. This complete 9.5 m high fresh section was generated by excavation of the pre-existing cliff to stabilise the former clay quarry that was restored in the late 1990s. Unfortunately, the section is no longer accessible, and our unpublished results from that early sampling will be reported here.

A succinct present-day vegetation survey was carried out in the three areas studied. The current vegetation has been heavily modified by urbanisation (roads, buildings) and human occupation (organic pollution, trampling). The Aleppo pine forest and the Mediterranean oak grove (*Quercus pubescens*, *Q. ilex*), highly degraded and sometimes limited to scattered individuals, are the only remnants of the natural forest vegetation that existed before the urbanisation of the Marseille basin [25]. Other plants are characteristic of ruderal environments disturbed by man (numerous Cichorioidae, *Plantago*, Poaceae, etc.),

cultivated (*Ficus carica*, *Punica granatum*) or invasive taxa (*Ailanthus altissima*), or have been planted for shade (*Platanus orientalis*, *Celtis australis*) or aesthetic appeal (*Cercis siliquastrum*).

(**A**) (**B**)

Figure 2. (**A**) Tufa cutting with a water-cooled circular saw; (**B**) sample of Saint Exupéry High School.

3. Materials and Methods

3.1. Palaeomagnetism

Palaeomagnetic investigations were conducted in the palaeomagnetic laboratory of the CEREGE. Oriented samples were retrieved using a Pomeroy core drill. Remanent measurements were performed using the superconducting rock magnetometer SRM760R (2G Enterprises). Stepwise alternating field (AF) and thermal demagnetisations were undertaken with the online AF demagnetisation system attached to the SMR760R and the MMTD Furnace (Magnetic Measurements Liverpool Ltd., Aughton, Ormskirk, UK). The 32 samples retrieved from the St Exupéry High School (SX), La Viste (CAM) and Calade (CAL) sections were subjected to AF demagnetisations. For the Plan d'Aou section (TRM), 14 pilot samples were subjected to stepwise thermal demagnetisations with interpretable results up to 350 °C (unpublished results obtained in 2002). The 32 remaining samples were measured after a single heating at 150 °C. Statistics on demagnetisation patterns were calculated using PuffinPlot Software, version 1.4.1 [26]. Magnetostratigraphic interpretation is based on ages reported in [27].

3.2. Sedimentologic and Petrographic Analyses

A sedimentologic analysis of the calcareous tufa (petrography, sedimentary structure and depositional facies) from three localities has been performed: Saint-Exupéry High School (Figure 3), La Calade (Figure 4) and La Viste (Figure 5). The depositional facies of the calcareous tufa have been classified using a continental carbonates facies nomenclature [28], which is based on the depositional texture, grain size and the nature of dominant carbonate components, such as phytoclasts, skeletal bioclasts, concoids and peloids. Additionally, four thin sections have been prepared from the Saint-Exupéry High School section and two from the La Calade section to characterise diagenetic and microstructural features of the tufa. Morphological and sedimentological features evidenced on the studied section have been used to define a conceptual model of the depositional palaeoenvironment for the calcareous tufa of the Marseille basin.

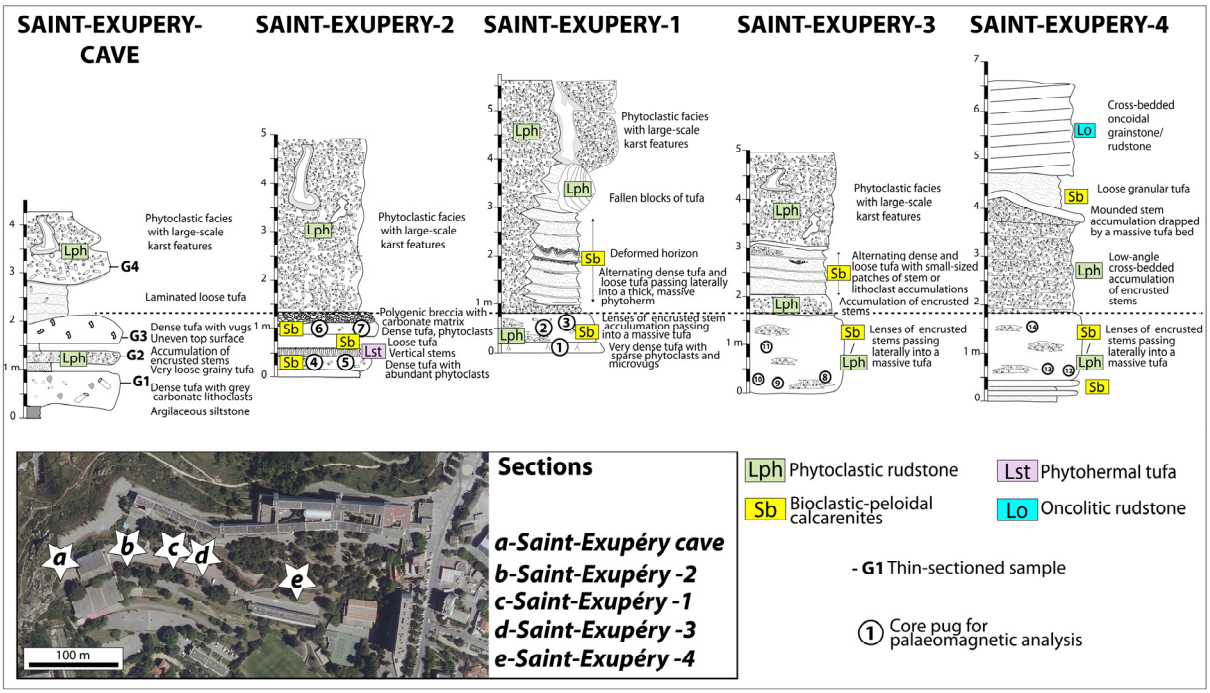

Figure 3. Sedimentary logs of various sections in the Saint Exupéry High School.

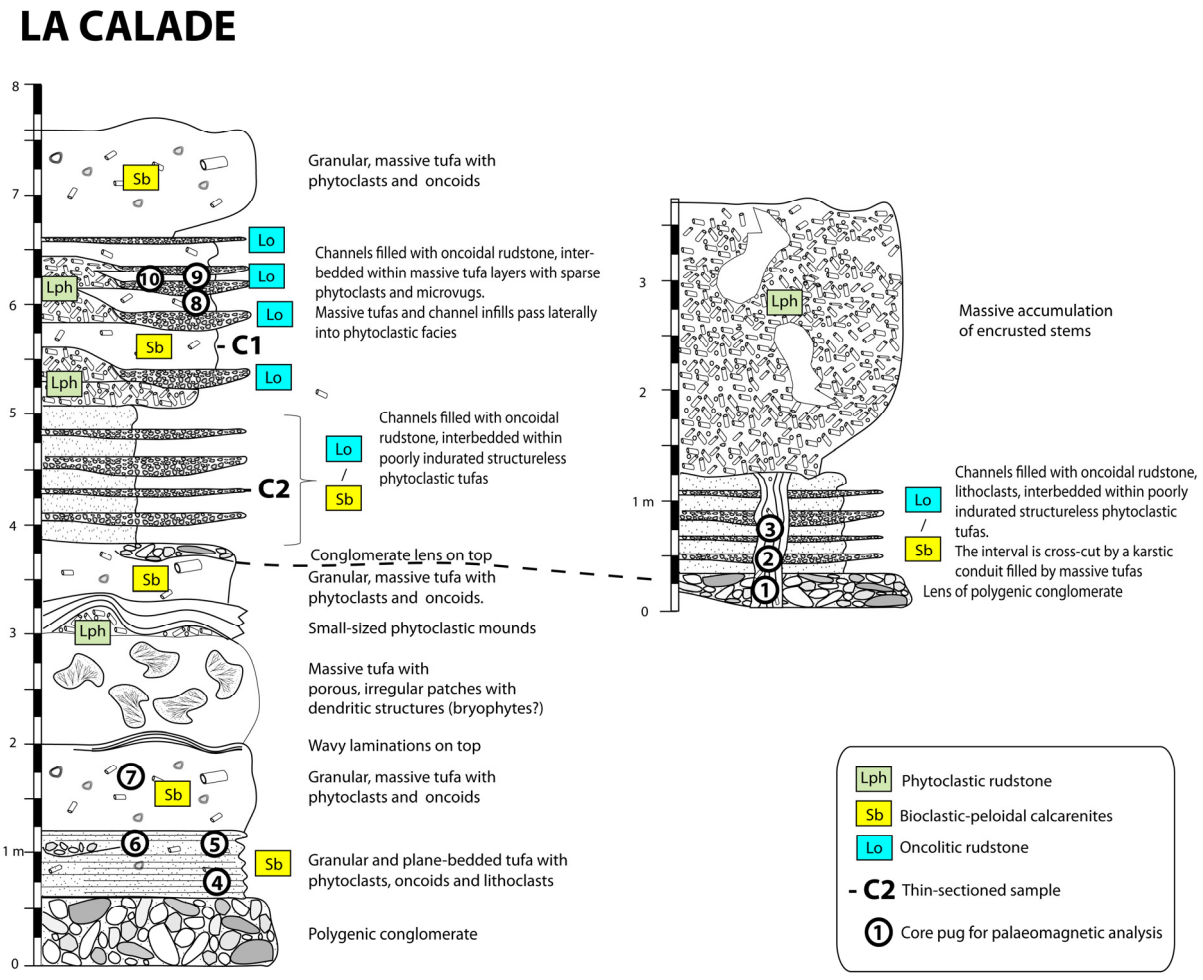

Figure 4. Sedimentary logs of La Calade section.

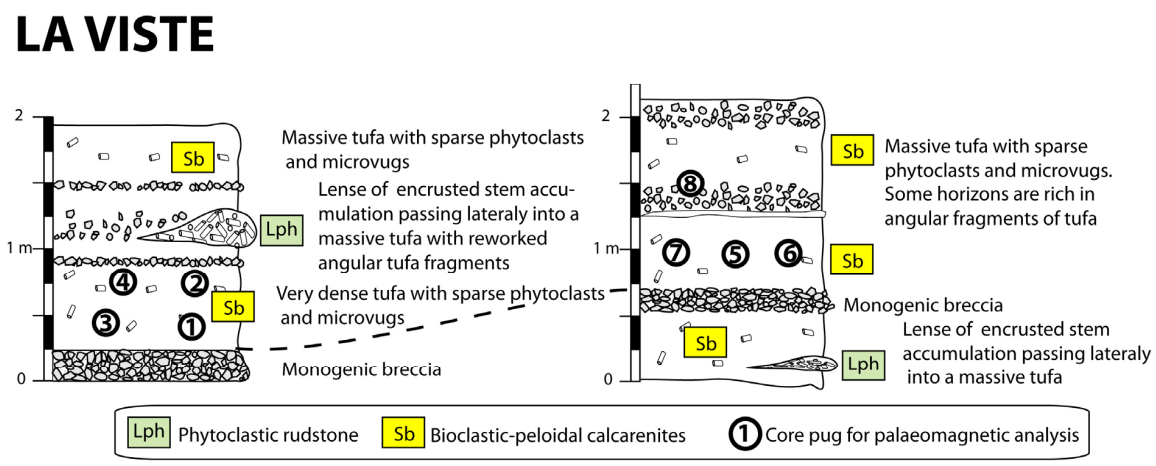

Figure 5. Sedimentary logs of La Viste section.

3.3. Carbon and Oxygen Stable Isotope Composition of Carbonates

Bulk stable carbon and oxygen stable isotope compositions of carbonate powders were measured to characterise the palaeohydrological setting of tufa formation. Carbonate rocks were samples from Saint-Exupéry High School (4 samples), La Calade (2) and La Valentine (19) sections. Previously published measurements from Les Aygalades [29] were integrated into the database. The location of sampled sections is displayed in Figure 1.

Measurements were taken at the GeoZentrum Nordbayern department, Friedrich-Alexander-Universität Erlangen-Nürnberg (Germany) through reaction with phosphoric acid at 70 °C using a Gasbench II connected to a Thermo Fisher Scientific DELTA V Plus mass spectrometer. All measured isotopic values are normalised against the international reference NBS-19 and are expressed in ‰ relative to V-PDB for 18O/16O and $^{13}C/^{12}C$. Mean external repeatability for $\delta^{13}C$ and $\delta^{18}O$ was better than 0.05‰ and 0.07‰, respectively.

3.4. Pollen and Non-Pollen Palynomorphs (NPP) Analyses

As travertine and tufa are known to be pollen-poor [18], we carried out pollen extraction on a sediment mass of between 50 and 250 g, using a technique that includes the use of a heavy liquor [30]. Carbonates were removed with concentrated hydrochloric acid, and organics were removed with 10% KOH and acetolysis (acetic anhydride and sulfuric acid). The separation of the pellet on heavy liquor composed of sodium heteropolytungstates (LST Fast Float diluted in water to a density of 2) removed residual mineral matter. The pellets were then passed through a 175 µm sieve, followed by a 10 µm filter.

Of the 23 samples taken, only 7 were polliniferous, corresponding to 6 different sites: La Viste, Saint-Exupéry High School, La Calade, Amaryllis, Les Olives quarry materials and Les Olives Avenue (Supplementary File S1). Observations were made with a light microscope (X 500 magnification), and identifications were made using photographic atlases [31–37], as well as a collection of pollen reference slides.

To identify the pollen of proto-cereals (with the exception of *Secale*, which is characteristic), we followed the following criteria: a longest diameter ≥40 µm, a large and protuberant annulus + pore and scabrate to verrucate surface sculpturing of the exine [5]. We are aware that some rare wild Poaceae may show a diameter ≥40 µm, such as *Aegylops* sp. and *Glyceria* sp., but the surface analyses carried out in Anatolia show that even in stations where these wild Poaceae are present, they are rarely or not represented in the pollen assemblages [5]. It therefore seems that their presence can be considered to be of little significance in a pollen assemblage. We have not attempted to identify cereal pollen down to the species level on the basis of morphometric criteria because we believe this is not possible due to their variable morphometry, which can depend on several factors, including the pollen mounting medium. Furthermore, in the determination tables, the sizes of pollen grains of different cereals may overlap [34].

The pollen of *Pinus halepensis* was identified in a single sample (Supplementary File S2) based on the presence of a marginal ridge on either side of the proximal thickness of the *Pinus* grain in equatorial view (cf. current *P. halepensis* pollen reference collection). In fossil pollen assemblages, this criterion is not always visible. It is therefore likely that *P. halepensis* pollen has been underestimated in the pollen counting. Mediterranean pine pollen includes *Pinus* grains > 63 mm long as *Pinus maritima*, *P. pinaster* or *P. pinea*. In pollen sample 5, *Platanus* is over-represented due to the presence of a piece of stamen; therefore, this taxon was excluded from the pollen sum for climatic reconstructions.

3.5. Pollen-Inferred Climate Reconstructions

To improve our knowledge concerning the evolution of the Mediterranean climate during a time interval and a region that has been poorly investigated to date, a multi-method approach has been tested to provide quantitative estimates of past climates [38–40]. Here, we propose to advance and compare five pollen-based climate reconstruction methods: (1) an assemblage approach, the modern analogue technique (MAT; [41]); (2) a transfer function, the weighted averaging partial least squares regression (WA-PLS; [42]); (3) and (4) the recent machine learning methods, including the boosted regression trees (BRT; [43,44]) and (5) the random forest (RF; [45,46]) and (4) the climatic amplitude method (CAM, [47]). These methods have been previously used for climate reconstruction focusing on different time periods in the Mediterranean region based on both terrestrial and marine pollen records [39,48–54].

The methods use the present-day environment to quantitatively reconstruct past climates derived from fossil assemblages. MAT functions by determining the degree of dissimilarity between past pollen assemblages and modern pollen data. By using squared-chord distance calculations, MAT selects a number of modern analogues for each fossil pollen assemblage to infer past climatic values [41]. In contrast to the MAT, which is an "assemblage approach", the weighted averaging partial least squares regression (WA-PLS) method is a true transfer function, meaning that it requires statistical calibration between the climate parameters and modern pollen assemblages. It is a regression method which supposes the unimodal relationship between pollen percentages and climate parameters [42]. WA-PLS and MAT methods are applied with the R package *Rioja* [52]. In comparison to the other methods, BRT and RF are new machine learning methods only recently adopted for palaeoecology [55]. These methods are based on a large number of regression trees and use random binary splitting and cross-validation to predict the relationship between climatic variables and pollen assemblages [54]. The machine learning methods have never been tested on periods older than MIS 11. RF is applied with the R package *randomForest* [55] and BRT with the R package *dismo* [56]. These four methods are based on a set of modern pollen data, including 1776 sites extracted from the Eurasian Pollen Dataset [38] and located between 11 °W and 58 °E and between 51 °N and 29 °N in order to encompass environments as similar as possible to the fossil pollen assemblages. For each method and climate parameter, performance statistics, including the coefficient of determination (R^2) and the root mean square error (RMSE), are presented in Supplementary File S3.

These methods have been developed mostly for recent time periods characterised by the absence of relict taxa. For older time periods, other methods can be more appropriate. In this frame, the outcome of these reconstructions will be compared to the results of the climatic amplitude method (CAM; Ref. [47]) that has been developed to quantify the climate of periods for which there are, currently, no modern analogues of the pollen spectra, such as the Pliocene and the Early Pleistocene. The CAM was developed to specifically quantify climatic parameters of the Mediterranean lowlands during the Late Cenozoic [47]. This method, which takes into account the modern bioclimatic requirements of taxa, is built on the statistical comparison between each past pollen assemblage and a database of more than 8000 modern pollen records from various latitudes and longitudes in the northern hemisphere, thus allowing the transposition of the relative abundances of each taxon into climatic values [47]. In the CAM, the most probable climate for a set of taxa corresponds

to the climatic range suitable for the maximum number of taxa. The climatic estimate is obtained as a climatic range and a "most likely value", which corresponds to a weighted mean, a statistical calculation tested on modern pollen data whose R^2 and RMSE values are given in Supplementary File S3.

Details of the development of all these methods have already been published, e.g., [39–43,45–47,50,53,57,58].

Here, six climatic parameters were reconstructed: mean annual air temperature (MAAT), mean temperature of the warmest month (MTWA) and of the coldest month (MTCO), mean annual precipitation (PANN), mean winter precipitation (Pwinter = December, January and February) and mean summer precipitation (Psummer = June, July and August). The precipitation seasonality is not reconstructed in the Climatic Amplitude Method. The reconstructed climatic values are compared to the modern climate of Marseille obtained from WorldClim 2 [59].

4. Results

4.1. Magnetostratigraphy

The intensity of natural remanent magnetisation (NRM) is weak, varying between 0.8 and 65 $\times$ 10^{-5} A/m but usually more than ten times above the magnetometer noise level (a few 10^{-5} A/m). Alternating field (AF) demagnetisation was complex to apply because the drift of the sample holder correction under AF treatment may be of the same order of NRM intensity. Therefore, we preferred to apply thermal treatment. The characteristic primary remanence (ChRM) was identified in between 100 and 250 °C because the signal tends to be scattered above these temperatures. We sometimes used a single heating step of 150 °C to remove an eventual goethite signal suggested by the yellow-beige color of the material, followed by AF demagnetisation. The component remaining above 150 °C is carried by fine-grained magnetite, as suggested by hysteresis ratios on five samples with Brc/Bc in between 2.5 and 3 and Mrs/Ms in between 0.05 and 0.16. Satisfactory demagnetisation plots were obtained in most of the samples (Figure 6), allowing to define a polarity. The interpreted reverse polarity of ChRM was sometimes derived from the great circle behaviour during demagnetisation rather than the principal component analysis. Note that no tilting correction was applied. When visible, the irregular bedding is roughly horizontal.

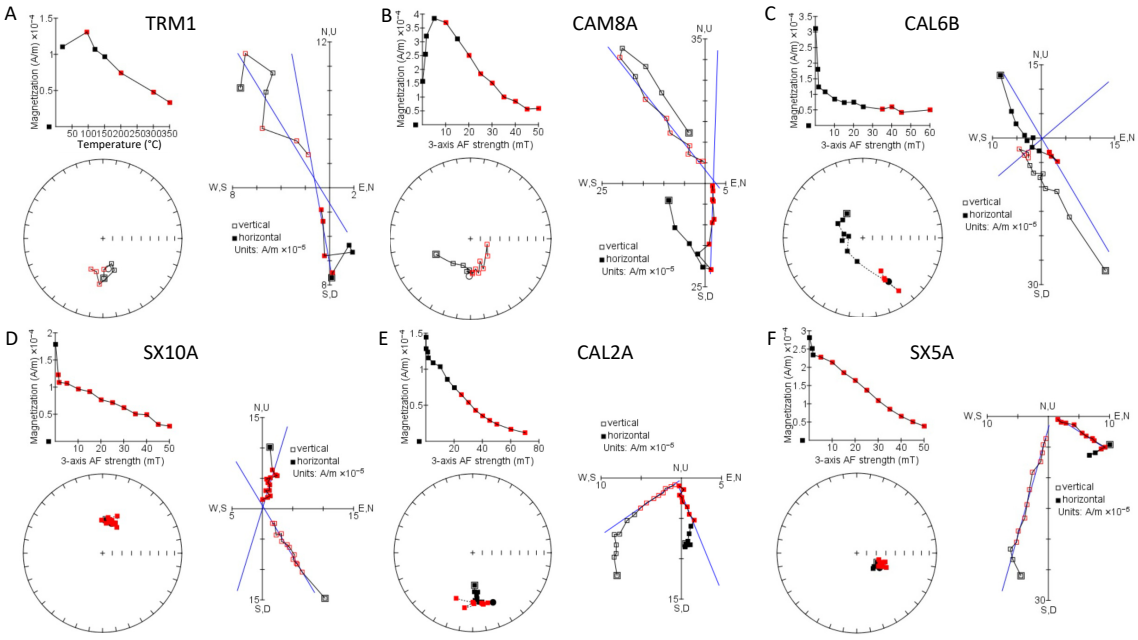

Figure 6. (**A**–**F**): Demagnetisation analyses for 6 representative samples. Full/open squares are upper/lower hemisphere for the equal-area plots' horizontal/vertical component on the orthogonal plots. Points used for calculation of ChRM directions are in red.

The 46 samples of the 9.15 m high Plan d'Aou section revealed a majority of reversed polarity (26), in particular in the first 3.6 m of the section, 8 normal polarities were mostly concentrated in the 6.4–7.3 m interval, while the remaining 12 'intermediate' (in fact, mostly undefined) directions mainly occur in the 3.75–5.6 m interval and above 7.3 m (Figure 7 and Supplementary File S4). The fact that the intermediate directions are intermingled with reverse directions in the upper 2 m leads to an interpretation of the whole section as belonging to the Matuyama period. A normal polarity seems robustly recorded over about one metre in the upper part of the section (6.3–7.35 m). Based on the chronological constraints from the reported Proboscidean remains, it is not possible that the observed normal polarity zone corresponds to the Olduvai subchron (1.77–1.93 Ma). Therefore, our preferred interpretation identifies the normal interval with the Jaramillo subchron (0.99–1.07 Ma). Assuming a constant deposition rate of 1.31 cm/ka, based on the apparent thickness of the Jaramillo subchron, the Plan d'Aou section would cover 0.7 Ma on the 0.85–1.55 Ma period. However, the assumptions made for this calculation (limits of Jaramillo, constant deposition rate) are quite poorly constrained, and we surmise that the actual period may be significantly shorter. Indeed, a cyclicity is clearly visible in the colour and porosity of the section, with at least four mega-cycles, visibly subdivided into smaller cycles (Figure 6). If these cycles correspond to the 100 ka glacial/interglacial cyclicity, it would point toward a circa 400 ka duration. However, we acknowledge that this cyclostratigraphic argument is debatable because that period is assumed to be dominated by a 40 ka cyclicity, and we offer it just as a potential narrowing of the palaeomagnetic estimated duration. Based on stratigraphic observations, the sites sampled for pollen analysis cannot be younger than the top of Plan d'Aou section. Accordingly, reverse polarity characterises all the samples of La Viste and a few samples of the La Calade site. The other samples with normal directions in Calade and all the Saint Exupéry samples would either belong to the Jaramillo subchron or correspond to a remagnetisation. Note that the stratigraphic heights of these new sections are quite limited, with irregular intervals; thus, correlation with the Plan d'Aou section is not feasible. Finally, it is worth noting that the base of the Calade site shows quite consistently declinations roughly heading south but with positive, sometimes very steep inclinations, with reasonable demagnetisation behaviour. This could be the result of the bulk rotation of a reverse polarity due to collapse toward the south of the whole hanging cliff in this zone that corresponds to a step descending southward to the sea (altitude difference between Calade and Saint Exupéry section bases is about 20 m). To summarise, these results, along with the mammal remains, indicate that all (but one; see discussion) obtained pollen-bearing samples are within the 0.85–1.55 Ma boundaries, likely to be narrowed around the Jaramillo subchron (e.g., 0.9–1.2 Ma).

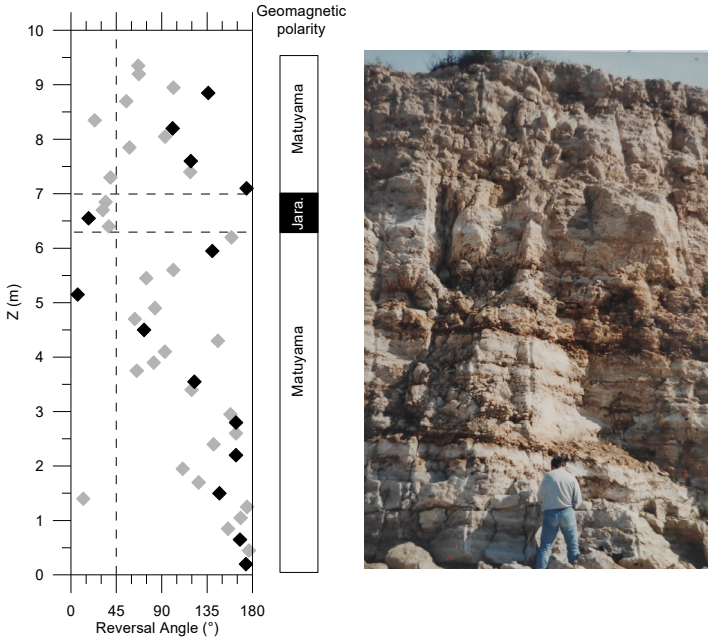

Figure 7. Reversal angle versus depth of the Plan d'Aou section, with picture of the section. Solid diamonds correspond to directions determined using full demagnetisation data, while grey diamonds correspond to a blanket demagnetisation at 150 °C.

4.2. Depositional Facies of Calcareous Tufa and Palaeoenvironmental Reconstructions

The analysis of outcrops and microfacies have allowed for the characterisation of the geomorphological landscape type that existed at the time of tufa formation. The sedimentary facies are diversified and show the alternation of carbonate and terrigenous facies, fluvial (tufa and conglomerate) and lacustrine-palustrine (compact, non-porous silt, encrusted reeds in live position). In total, the different sedimentary logs have allowed the observation of four groups of tufa facies: (1) phytoclastic rudstone (Lph), (2) bioclastic-peloidal calcarenite (Sb), (3) phytohermal tufa (boundstone of stems: Lst1) and (4) oncolitic rudstone/floatstone (Lo). Such a facies association has been reported in various temperate climate settings and has been shown to characterise distinct hydrodynamic settings within a fluvial environment [28,60]:

- Phytoclastic rudstones (Lph) consist of an accumulation of coated stems (centimetre- to decimetre-long) with a scarce peloidal micrite matrix. Phytoclastic rudstone form up to 4 m high domes, sometimes with subvertical walls (Figure 8B). They develop through calcite precipitation around plants. These plants may be transported before encrustation, thus forming a dam. Plant accumulations are believed to initiate dams around obstructions or slope breaks. Phytoclastic rudstones (Lph1) commonly pass laterally to calcarenites (Sb) (Figure 8B).
- Bioclastic-peloidal calcarenites (Sb) are fine-to-medium grained carbonate sands. Grains predominantly consist of peloids, intraclasts (broken calcitic crusts), micro-oncoids and bioclasts (dominantly ostracods, more occasionally molluscs). They are organised into centimetric to decimetric thick beds with horizontal laminations (Figure 8B,C). They are interpreted as forming in slow-flowing dammed areas.
- Photothermal tufa (Lst) are boundstones of in situ stems (mainly reeds) growing upward. Stems are commonly decimetre-long and exhibit thick (up to few centimetres) calcite coatings (Figure 8A). They form in palustrine settings on fluvial banks or lake shores.
- Oncolitic rudstone (Lo) are formed by an accumulation of oncoids (typically less than 1 cm in diameter). They are organised into decimetre-thick lenses displaying an erosive base (Figure 8C) and commonly exhibit cross-stratification. They are interpreted as representing fluvial channel fills.

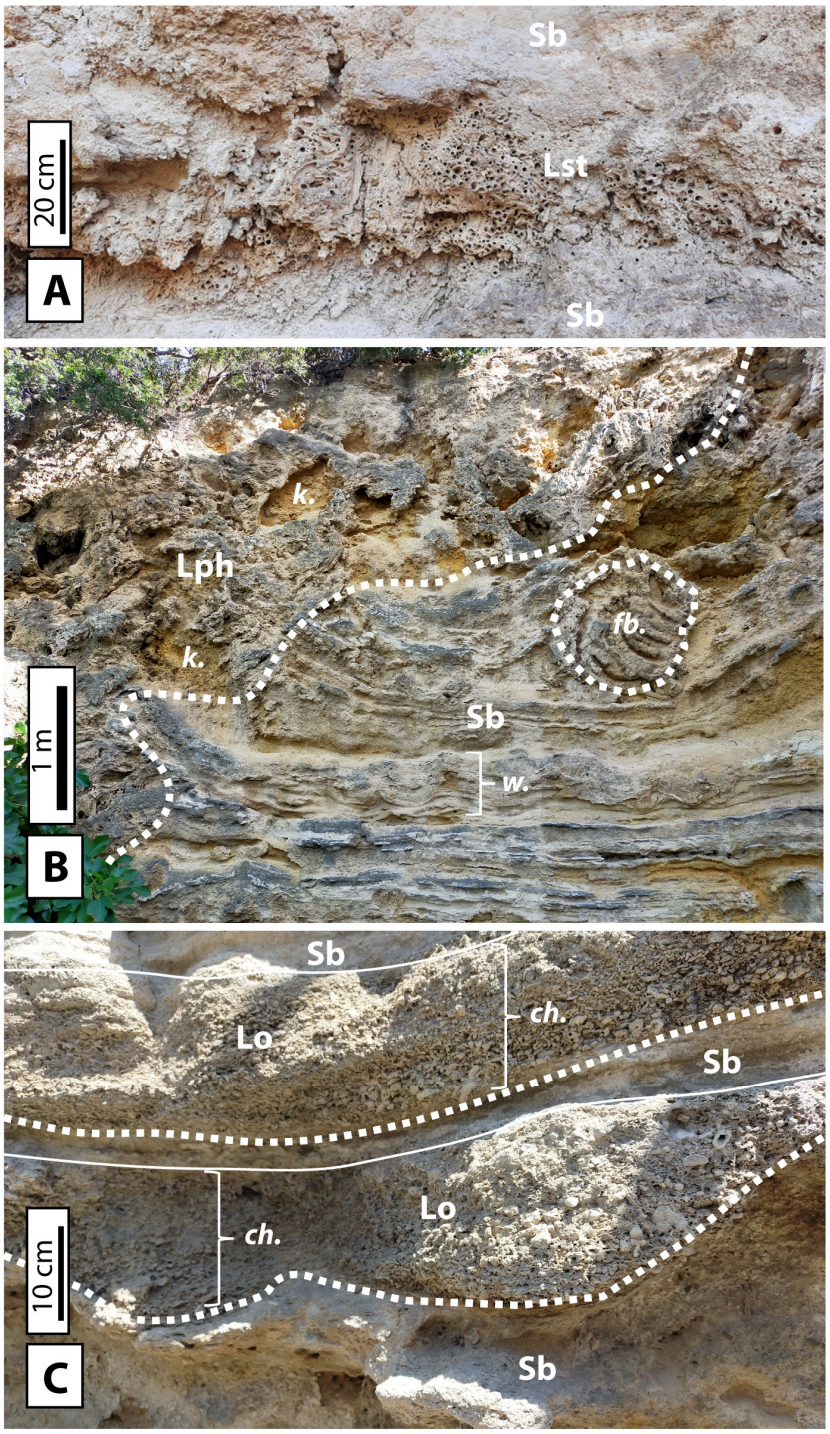

Figure 8. Pictures of tufa outcrops in the Marseille basin. (**A**) Saint-Exupéry High School: phytohermal tufa (**Lst**) with coated vertical stems of reeds (cf. *Phragmites*), interbedded with calcarenitic tufas (**Sb**). (**B**) Saint-Exupéry High School: high-relief barrage formed by the in situ calcite coating of accumulated plant fragments (Phytoclastic rudstone: **Lph**). This barrage is onlapped by cm- to dm-thick layers of calcarenitic tufas (**Sb**), some of them displaying a wavy bedding (***w.***) resulting from soft sediment deformation processes. A block of phytoclastic rudstone (***fb.***), likely fallen from the steep barrage wall, is encased within **Sb** tufas. Karstic cavities (**k.**) are common within phytoclastic tufas. (**C**) La Calade section: oncolitic rudstones (**Lo**) infilling channels (**ch.**), incising calcarenitic tufas (**Sb**).

The rivers in which these tufa formations develop originate from sources located within the Marseille basin itself at the foot of the Etoile, La Nerthe or Allauch massifs. The intercalations of terrigenous facies (e.g., polygenic conglomerates at Saint-Exupéry High School and La Calade sections: Figures 3 and 4 show that rivers with larger catchment areas transport elements resulting from the erosion of neighbouring massifs, coexisting in the Marseille basin with rivers originating from more localised sources.

Based on palaeoenvironmental interpretations of facies, a conceptual depositional model for the Early Pleistocene continental sedimentation in the Marseille basin is proposed in Figure 9.

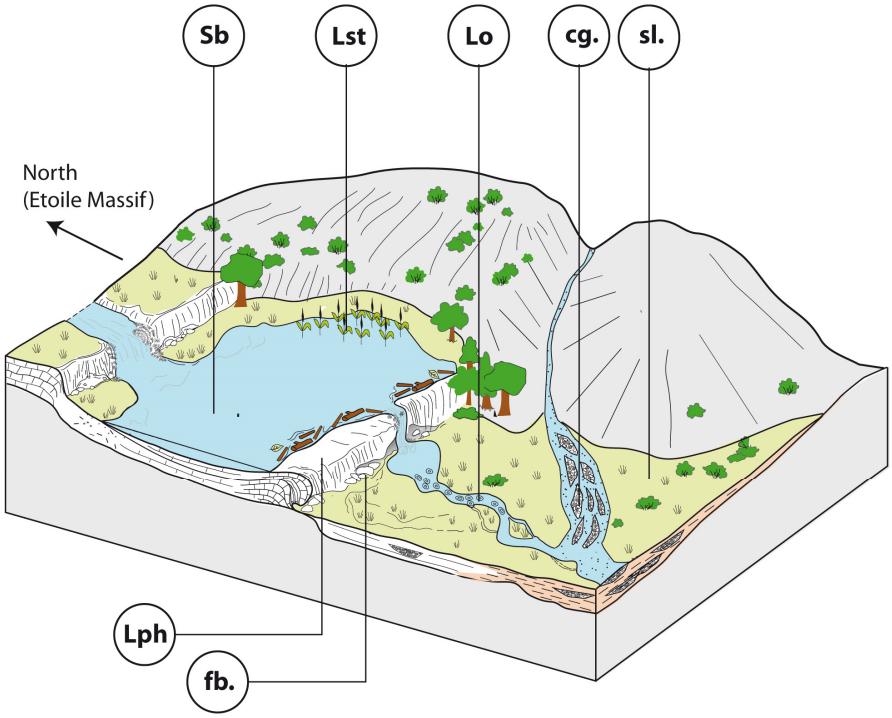

Figure 9. Conceptual depositional model for the lower Pleistocene continental sedimentation in the Marseille basin (adapted from [28]). **Lph**: phytoclastic rudstone (barrage); **Lst**: Phytohermal tufa (paludal environments with reeds); **Sb**: bioclastic-peloidal calcarenites (low-to-medium energy dammed environments); **Lo**: oncoidal rudstones (channel fills); **cg.**: conglomerates (braided channel fills or bars); **sl.**: silts (floodplain); **fb.**: fallen blocks.

Finally, the very negative range of $d^{13}C$ values (Figure 10 and Supplementary File S5) measured in the Pleistocene tufa from the Marseille basin (from −2.9 ‰ to −9.8‰ PDB) is consistent with that of calcareous tufa, formed in cool water, and is clearly distinguished from that of travertine, formed from hot water of hydrothermal origin [60,61].

The very reduced range of both $\delta^{13}C$ and $\delta^{18}O$ values in Les Aygalades, Saint-Exupéry and the La Calade section (northern Marseille basin) suggest very short water residence times and limited evaporative ^{18}O enrichment, which is consistent with flowing water [62]. In contrast, with regard to the wide range of $\delta^{13}C$ and $\delta^{18}O$ values in the La Valentine section (eastern Marseille basin), their overall covariant trend would indicate longer residence times and dominantly lacustrine conditions [63].

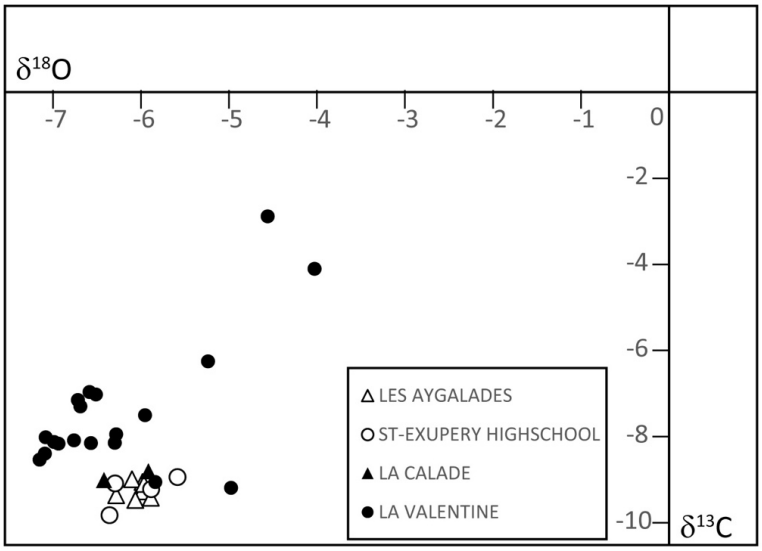

Figure 10. $\delta^{13}C$ vs. $\delta^{18}O$ cross-plot of bulk carbonates from calcareous tufa from the Marseille basin (see Figure 1 for location of sampling localities).

4.3. Pollen and NPP Data

The total number of taxa identified (this study and former macro-remains studies [13,23] is 122 (Table 1), of which 91 are pollen, spores, NPPs and algae, and 32 are plant macro-remains. A classic classification to name organisms was used [64].

Spores and NPPs have been excluded from the pollen sum (PS) for the calculation of relative frequencies. In this case, the mean PS is 117 grains per sample. When spores and NPPs are included, the mean PS per sample is 27,096. The average pollen concentration (weighting method, [29] is 244 pollen/g sediment (minimum: 2, maximum: 468). In total, 92 pollen taxa were identified, including 36 trees, 45 herbs and 11 NPPs (Supplementary File S2, Figures 11 and 12). Despite their low average pollen concentration, we consider that the samples studied are ecologically valid because of their taxonomic diversity (e.g., [65]). Simplified pollen diagrams (Figures 13–15) were drawn with C2 [66]. The ecological classification of pollen taxa used to draw the pollen diagram is summarised in Supplementary File S6.

The proportion of arboreal pollen varies between 50 and 85% of the pollen sum, indicating that the landscape was not entirely forested, with open areas which could be dry grasslands on Oligocene and Cretaceous limestone hills surrounding the tufa sites or wet grasslands in depressions crossed by watercourses (Figures 13–15). Trees are dominated by pine woods, including Mediterranean pines and oak woods. Within the steppe, we find the classic associations with *Artemisia* sp., Chenopodiaceae, numerous Compositae species and Poaceae.

Aquatic and riverine plants indicate that a riparian forest had developed along the streams that flowed near the tufa. This riparian forest was diverse and different from the one which exists today on the French Mediterranean coast. It included *Alnus glutinosa*, *Corylus*, *Fraxinus*, *Populus* or *Salix*, as well as *Juglans* and *Platanus*, whose geographic distribution is now east Mediterranean. The extreme rarity of tertiary mega-thermophilous taxa in floristic assemblages is interesting because elsewhere in the western Mediterranean, such as in the Baza Basin (SE Spain), *Carya*, *Pterocarya*, *Eucommia*, *Parrotia*, *Tsuga* or *Cataya* are maintained in the 1.2–1.5 Ma period [67]. Their absence from Marseille may be either taphonomic or climatic in origin. Alternatively, it may point toward a younger age interval for the Marseille tufa samples, as already pointed to in the palaeomagnetic interpretation.

Coprophilous NPPs were mainly found in samples 1 and 7. These included *Delitschia*, *Sordaria*, *Valsaria* and Type 200, which can be abundant in grazed areas [68]. Cerealia pollen was found in these samples, with Cerealia counts in sample 1 being the highest of all the pollen spectra studied. Nitrophilous plants can reach significant values (32% of PS) as in

sample 2 (Figure 13), where Cerealia is also noted. This is a further indication of the impact of herds of large herbivores on ecosystems.

The pollen data show strong variability, particularly between oak forest and steppe. This variability could indicate that several climatic phases are recorded, marked by alternating temperate and cooler phases. The stratigraphic position of sample 7 is just below the tufa with an unknown age control (although assumed to be Pleistocene). As the pollen assemblage of this sample is consistent with the six tufa pollen samples, we consider that sample 7 is contemporary with the deposition of the Marseille tufa.

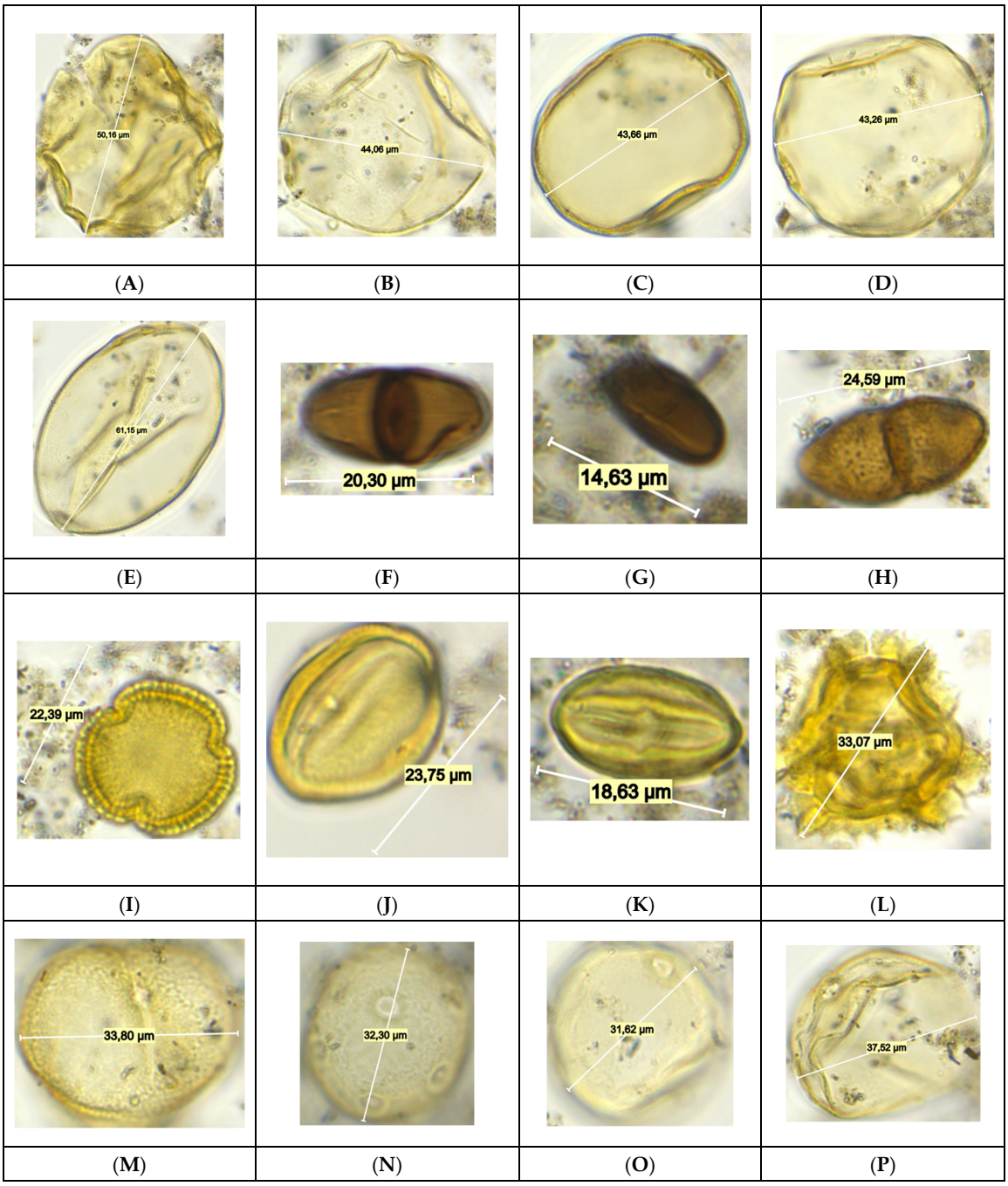

Figure 11. (**A**) Cerealia L = 50.16 µm; (**B**) Cerealia L = 46.02 µm; (**C**) Cerealia L = 43.66 µm; (**D**) Cerealia L = 43.26 µm; (**E**) *Secale* sp. L = 61.15 µm; (**F**) *Delitschia* L = 20.3 µm; (**G**) *Coniochaeta* L = 14.63 µm; (**H**) *Valsaria* sp. L = 24.59 µm; (**I**) *Olea* sp. L = 22.39 µm; (**J**) *Vitis* sp. L = 23.75 µm; (**K**) *Castanea* sp. L = 18.63 µm; (**L**) Cichorioideae L = 33.07 µm; (**M**) Rumex sp. L = 33.8 µm; (**N**) Plantago lanceolata sp. L = 32.3 µm; (**O**) Poacaeae L = 31.62 µm; (**P**) Poacaeae L = 37.52 µm.

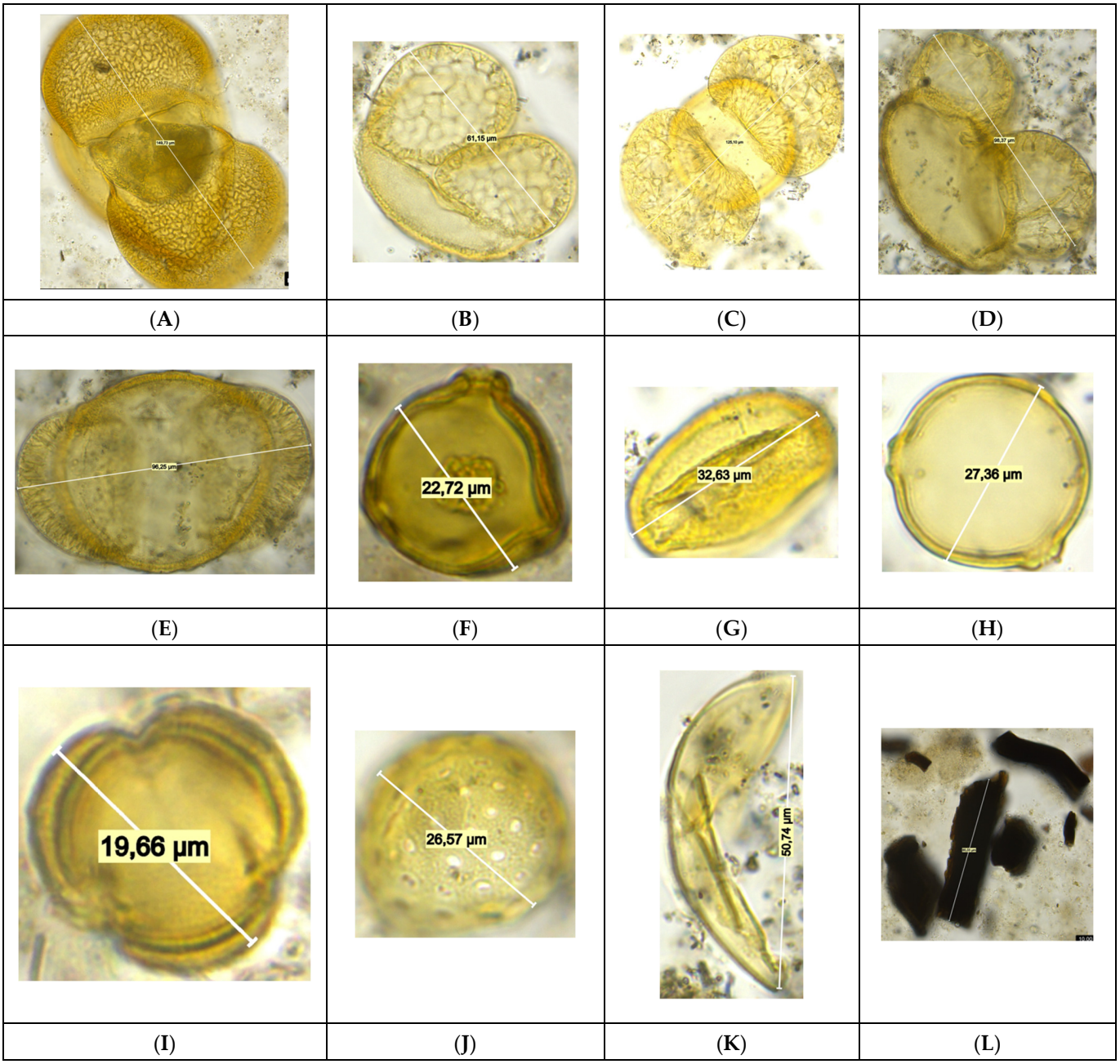

(**A**) (**B**) (**C**) (**D**)

(**E**) (**F**) (**G**) (**H**)

(**I**) (**J**) (**K**) (**L**)

Figure 12. (**A**) *Picea* sp. L = 149.73 µm; (**B**) *Pinus sylvestris* sp. L = 61.15 µm; (**C**) *Abies* sp. L = 125.10 µm; (**D**) Mediterranean *Pinus* L = 98.37 µm; (**E**) *Cedrus* sp. L = 96.25 µm; (**F**) *Betula* sp. L = 22.72 µm; (**G**) Deciduous *Quercus* L = 32.63 µm; (**H**) *Ostrya/Carpinus orientalis* L = 27.36 µm; (**I**) *Artemisia* sp. L = 19.66 µm; (**J**) Chenopodiaceae L = 26.57 µm; (**K**) *Juniperus* sp. L = 50.74 µm; (**L**) *Charcoal* sp. L of the longest = 85.03 µm.

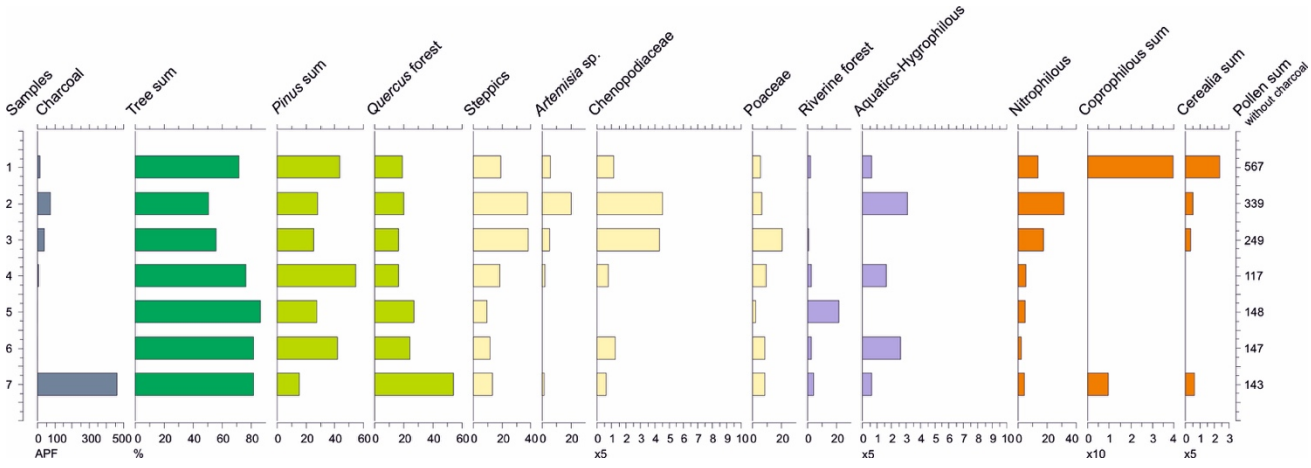

Figure 13. Synthetic pollen diagram of the Marseille tufa.

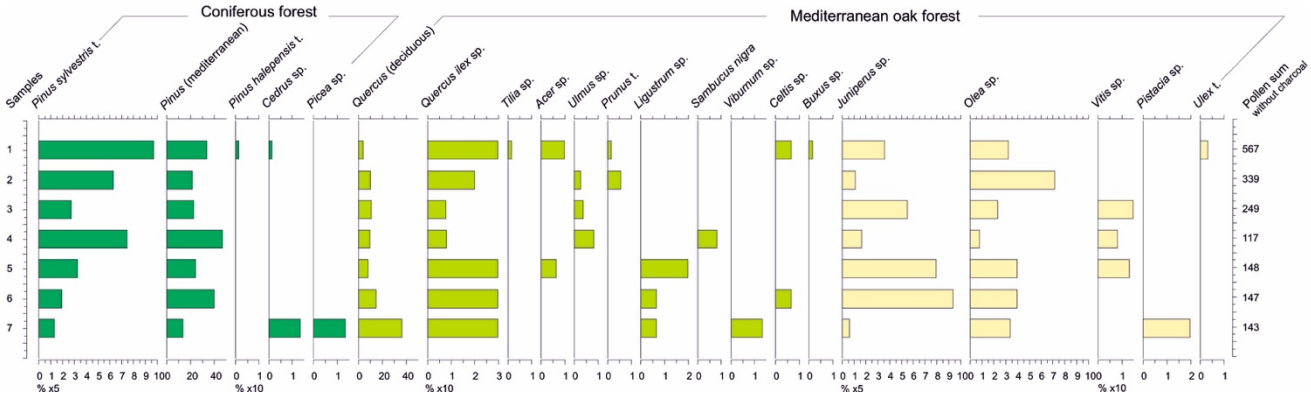

Figure 14. Synthetic pollen diagram of the Marseille tufa: trees 1.

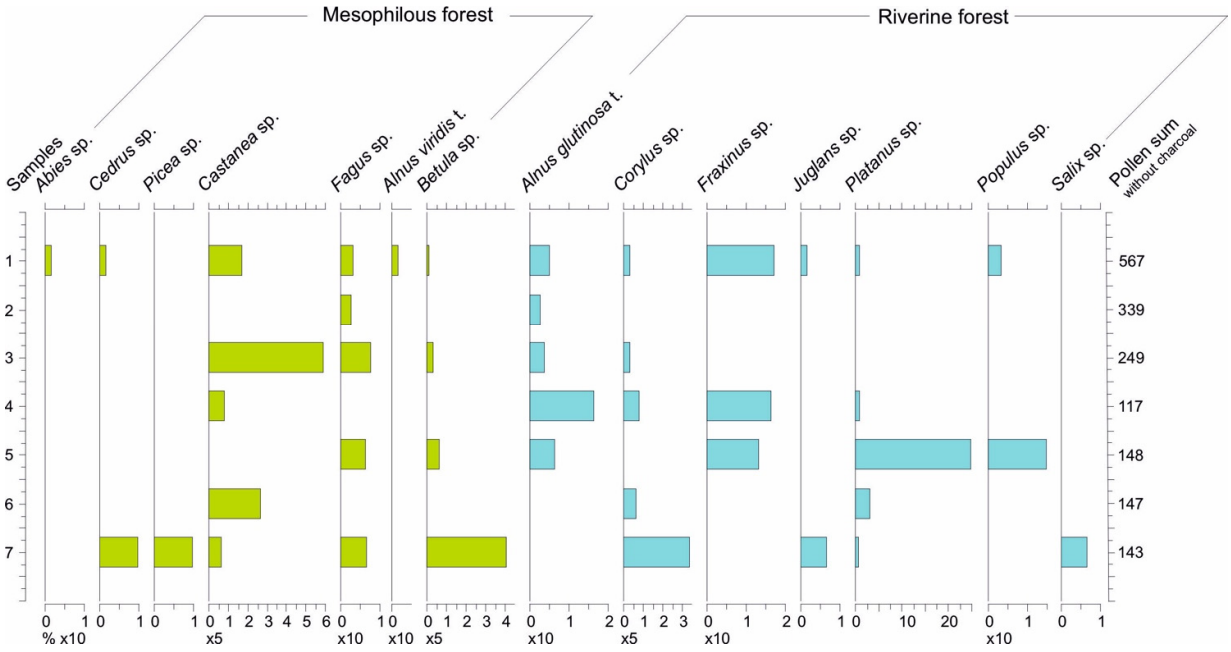

Figure 15. Synthetic pollen diagram of the Marseille tufa: trees 2.

4.4. Pollen-Inferred Climate Reconstructions

Pollen-inferred climate reconstructions of the Marseille basin were conducted using a multi-method approach (Figure 16). The model performance of the different methods shows the best values, with the higher R^2 and lower RMSE for the BRT method for all climatic parameters (Supplementary File S3). The differences between the reconstructed climate values from each method can be important. For temperatures (MAAT, MTWA, MTCO), the mean difference between the different methods corresponds to 4.2 ± 1.2 °C. The MAT, WA-PLS and RF methods reconstruct close values, with a mean difference of 1.5 ± 0.8 °C between the three methods. BRT shows close values, except for samples 4 (La Calade) and 6 (Les Olives quarry materials), where this method reconstructs higher values compared to MAT, WA-PLS and RF. The climatic amplitude method also reconstructs higher temperatures compared to the other methods. For precipitation (PANN, Pwinter, Psummer), the mean difference between the different methods corresponds to 208 ± 84 mm, 67 ± 24 mm and 53 ± 24 mm, respectively. Reconstructed precipitation tends to be higher in summer for WA-PLS and in winter for BRT, compared to the other methods.

Reconstructed MAAT shows a mean of 11.8 °C and varies between 8.8 and 15.8 °C for the different samples and methods used. Reconstructed PANN shows a mean of 729 mm.year^{-1} and varies between 447 and 981 mm.year^{-1} for the different samples and methods used. Reconstructed temperatures generally indicate colder conditions compared to modern values, particularly during winter, and reconstructed precipitation indicates wetter conditions compared to modern values. Differences do seem to be present between some samples. In particular, sample 2 (La Viste 2021) appears to differ with lower precipitation and higher temperatures compared to the other samples. The reconstructed values for this sample are closer to modern values, except for winter temperatures.

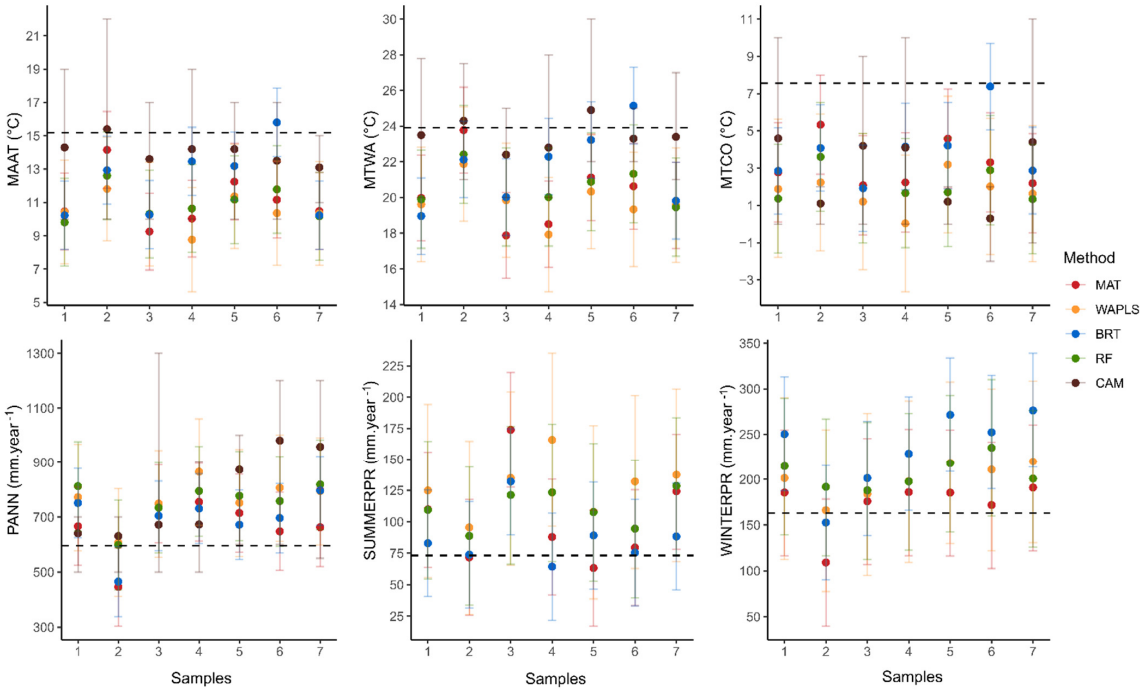

Figure 16. Pollen-inferred climate reconstructions of tufa samples from Marseille are based on five methods: MAT (modern analogue technique), WA-PLS (weighted averaging partial least squares regression), RF (random forest), BRT (boosted regression trees) and CAM (climatic amplitude method). Six climatic parameters have been reconstructed: MAAT (mean annual air temperature), MTWA (mean temperature of the warmest month), MTCO (mean temperature of the coldest month), PANN (mean annual precipitation), Pwinter (mean winter precipitation) and Psummer (mean summer precipitation). The error bars indicate the root mean square error (RMSE). Dashed lines correspond to modern climate values of Marseille's samples obtained from WorldClim 2 [59].

5. Discussion

5.1. A Diversified Geomorphological and Hydrological Landscape

Palaeoenvironmental reconstructions (Figure 9), based on sedimentary facies analysis, suggest that the Marseille basin was traversed by streams with carbonate sedimentation, likely originating from the foothills of the Mesozoic limestone massifs that border the basin to the north and east. These streams were interrupted by natural dams formed by accumulations of plants, stabilised by carbonate precipitation, thereby promoting the development of upstream water bodies with low hydrodynamics and even marshy environments. Other streams with wider catchment areas occupied the Marseille basin, forming braided channel systems with coarse, conglomeratic, terrigenous sedimentation.

These various types of streams carved through the clay-dominated Oligocene formations of the Marseille basin, forming a hilly relief. Over the past million years, due to tectonic movements, fluvial erosion and eustatic changes, a reversal of relief has occurred [6]. The calcareous tufa plateau now stands prominently, rising 180 m above sea level, while the Oligocene clay hills, eroded by streams with carbonate sedimentation, are now visible beneath the tufa.

5.2. A mosaic of Mediterranean Vegetation

Biological data show that the vegetation landscape was dominated by a diverse Mediterranean vegetation, including mixed coniferous forest (*Pinus*, *Abies*, *Picea*, *Cedrus*), deciduous forest (mainly *Quercus*) and steppe with Poaceae, *Artemisia* and Chenopodiaceae.

In the pine forest, *Pinus nigra* subsp. *salzmannii* (Supplementary File S2) is present but is now only found in southern France from the Rhône valley to Roussillon [69], while other populations exist in Spain [70]. This tree was present in the Bouches-du-Rhône region until the end of the Middle Pleistocene [19], but its range shrank considerably during the Holocene as a result of competition from *Quercus ilex* and *Pinus halepensis*, favoured by human beings [71]. Palynologically, the pollen of *Pinus nigra* subsp. *salzmannii* is indistinguishable from that of *Pinus sylvestris*. It could therefore not be separated from the tufa samples by pollen count. *Pinus halepensis* was identified in pollen assemblages and plant macro-remains. Today, it is dominant in Provence on limestone soils frequently burnt by man. This tree, whose indigenous status has often been disputed and even attributed to the Romans, was also recorded in the Early Pleistocene in the Baza basin [67]. Other Mediterranean pines, whose pollen could only be identified to the genus level, may have been present in the Marseille basin, such as *Pinus pinea*, which could grow in the sandy, well-drained soils of the coast or the dolomitic outcrops of the Marseille basin, and *Pinus pinaster*, which could grow in acidic soils, such as those that may have formed on the Oligocene clay hills.

The oak forest was diverse, with many species typical of north Mediterranean *Quercus* forests, including *Tilia* sp., *Acer* sp., *Ulmus* sp., *Prunus* t., *Ligustrum* sp., *Celtis* sp. and *Buxus* sp. The presence of *Vitis* sp., a liana very often associated with oak in the Mediterranean region, is also noteworthy. According to the macrorests [23], this *Vitis* is the species *V. vinifera* subsp. *sylvestris*, the ancestor of the cultivated vine. On south-facing slopes, woody plants such as *Olea* sp. and *Pistacia* sp. could grow, as well as *Ulex* (probably *U. parviflorus*, which dominates the garrigue of Bouches-du-Rhône) and *Juniperus* (*J. oxycedrus*, *J. phoenicea*). This heliophilous community could also include heathers such as *Erica multiflora*, a flowering heather that thrives in carbonate soil and whose distribution is currently limited to the coast because it is frost-averse, and *Erica arborea*, an acidiphilous heather that is tolerant of calcareous soils. *Erica arborea* was also able to take advantage of the acidic soils that had developed on the Oligocene clays.

In the cooler, valley-bottom or north-facing areas, mesophilous forests could develop. These included taxa that have now practically all disappeared from the Marseille basin or have become very rare. These include *Abies* (Figure 12C), *Cedrus* (Figure 12E), *Picea* (Figure 12A), *Castanea* (Figure 11K), *Fagus*, *Alnus viridis* and *Betula* (Figure 12F). The presence of *Castanea* is singular for a calcifuge tree that disperses its pollen very little. Its

presence is highest (6% of PS) in the sample from the Saint Exupéry High School section (sample 3), located just above the thick layer of Saint Henri Oligocene clays. These clays are decarbonated. One Ma ago, they were outcropping and dominant everywhere in the Marseille basin. Acidiphilous populations of *Castanea* therefore benefited from an extensive biotope suited to the growth of a chestnut forest. These populations have been considerably reduced in the Marseille basin due to urbanisation, but a few plants remain as refuges on sites with acid soils, including St Marcel, Vallon de la Barrasse and Aubagne [72]. The *Cedrus* record is interesting because the native populations of cedar (*Cedrus atlantica*) closest to Marseille are currently found in North Africa (Morocco, Algeria). In the Early and Middle Pleistocene, *Cedrus* was more widely distributed in the western Mediterranean [67,73–76], appearing alongside *Pinus*, *Picea* and *Abies*, as in the Marseille calcareous tufa samples, and disappeared from the northern Mediterranean region through increasingly severe glacial–interglacial cycles [77]. *Picea* is recorded in sample 7. Its presence is not unusual in the Mediterranean basin because it is found in other Early Pleistocene records from southern Italy [74] and Spain [67]. An increase in aridity could be the cause of its disappearance in the Early Pleistocene [78]. In southern France, this taxon is poorly represented in pollen records [25,79], but it is still found in the Upper Holocene in the Calanques de Cassis [79]. *Abies*, whose presence is only noted in sample 1, is a tree found throughout the Pleistocene at low altitudes in the French Mediterranean [25]. Because of the low dispersal capacity of its pollen by wind and the short drainage basin of the rivers, *Abies* is considered to have been present at low altitude in the Marseille region. The question is "which *Abies*?" *Abies alba* is the only *Abies* currently present in the French flora but whose distribution is essentially sub-alpine, or is it another *Abies*, such as *Abies pinsapo*, found in Andalusia, or some other *Abies* species found in the eastern Mediterranean. It should be noted that in Europe the greatest taxonomic diversity of the *Abies* genus is found around the Mediterranean basin [80]. *Fagus* is found in almost all of the tufa samples. Like *Abies*, *Fagus* does not disperse its pollen widely and has remained in low-altitude areas of Provence until recently [25]. This tree has practically disappeared from the low-altitude areas of the Marseille basin, but a few individuals remain along the Huveaune river and at higher altitudes in the Sainte Baume massif, 25 km east of Marseille [72]. The very sharp contraction in the range of these taxa, or their disappearance from low-altitude areas, is most likely due to the combined action of man (agriculture, pastoralism, fires) and climate. This dynamic occurred during the upper half of the Holocene when the climate became cooler and drier and agricultural activities increased along with the human population. It is also possible that the Mistral, the powerful northerly wind that cools Rhodanian Provence in winter and dries out the soils all year round, was less vigorous in the Early Pleistocene than it is today.

The riparian forest that was established along the watercourses included *Juglans*, *Platanus*, *Alnus*, *Salix*, *Corylus*, *Fraxinus* and *Vitis*. The presence of *Platanus* and *Juglans* is unusual because these trees are no longer present in the riverine forests of Western Europe. They are found, on the other hand, in the eastern Mediterranean, Greece and Turkey. Bibliographic data show that these taxa were present in the Early Pleistocene and, even before, in the Pliocene [23] in the western Mediterranean basin in Spain and Italy [67,73,74,81,82] as well as on the French Mediterranean coast at low altitude [80]. They appear to be persisting until the end of the Holocene [25,79,83–86], in which the intensification of agriculture, increased use of water and the development of waterways are making them disappear.

In wetlands, populations of phragmites represented by abundant encrusted fossils (Figure 8A) were established. Pollen data show that there was also *Mentha* and *Iris*. In the waterways, there was probably a varied diversity of aquatic plants, but we only found *Myriophyllum spicatum,* which is an aquatic plant of ponds and rivers that likes basic soils rich in organic matter. Freshwater algae have been identified, including Chrysophyceae and *Botryococcus*. The populations of these algae explode when the aquatic environment is

disturbed, leading to eutrophication of the waters. The low representation of these algae in the assemblages shows that the trophic state of the aquatic environment was in equilibrium.

The herbaceous strata included steppe plants, adapted to dry and drained soil. Among these plants, *Artemisia* and Poaceae are dominant alongside Chenopodiaceae and many Compositae (*Anthemis*, *Aster*, *Centaurea cyanus*, *C. nigra*, Cichorioideae, *Cirsium*). Note that the Poaceae could include species linked to watercourses or bodies of stagnant water. The steppe could also contain proto-cereals and nitrophilous plants including *Plantago lanceolata*, *P. coronopus*, *Rumex* sp. and *Urtica* sp.

5.3. The Early Appearance of Proto-Cereals

The major finding of this study is the discovery of cereal pollen (Figure 11A–E). This discovery allows us to date the presence of proto-cereals on the northwestern shore of the Mediterranean back to ca. 1 Ma. In NE Spain, large (>40 µm) Poaceae pollen, which could be proto-cereals, were found in the Lower-Middle Pleistocene site of Cal Guardiola [80]. It is the only site in the western Mediterranean, together with the tufa layers of Marseille, which shows the occurrence of these taxa in such ancient times. In the eastern Mediterranean, proto-cereal pollen appeared in the Acıgöl lacustrine series at the beginning of the Lower Pleistocene from 2.3 Ma, making SW Turkey the earliest area for the presence of proto-cereals. In Marseille, these pollen types are accompanied by fairly high percentages of pollen from nitrophilous plants (Figure 13), such as *Plantago* (*P. coronopus, P. lanceolata, P. major/minor*), Cichorioideae, Chenopodiaceae, *Urtica, Rumex* and *Malva*. We observe spores of coprophilic fungi, such as *Delitschia*, *Sordaria*, *Valsaria* or Type 200 (Supplementary File S3; Figure 11F–H). These fungi have the particularity of completing their biological cycle in the excrement of large herbivores. It is possible that this nitrophilic and coprophilic assemblage was favoured by herds of large herbivores, which could be attracted by the freshwater resource of the tufa to drink and benefit from green pasture. This is often the case in regions of tropical tree savannahs frequented by herds of large herbivores.

In the Acıgöl series, where this biological configuration is also recorded [5], we proposed the same hypothesis to explain the early appearance of proto-cereals and propose that it is through trampling, grazing and the nitrogen enrichment of soils relating to herbivore droppings that genetic mutations may have occurred in the genome of wild Poaceae, leading to the appearance of cereal-type Poaceae with large pollen and seeds. The new discovery of proto-cereals in Marseille one million years before the start of the Neolithic confirms the hypothesis that we proposed in 2021 [5] and shows that it is well before the start of agriculture that proto-cereals were present in semi-wooded Mediterranean ecosystems and that it may be the disturbances generated by large herbivores that are at the origin of their emergence. Hominins, who became farmers, were therefore not responsible for the appearance of cereals. Cereals were already present in steppe ecosystems when agriculture became widespread in southwestern Asia in the Lower Pleistocene [87].

5.4. Potential Food Resources

A list of edible plants (Supplementary File S7) was established from the biological data presented in this article. In total, 82 edible taxa were identified (Supplementary File S7) based on our knowledge [5] and those found in the literature [88–91]. Among these plants, 49.3% are trees and 50.7% are herbs (Figure 17A,B). In the Acıgöl series (SE Turkey) where the steppe is dominant, edible plants are mainly herbs (Figure 17D). In Marseille and Acıgöl, the plant organs that could be consumed the most are the vegetative part of the plant (60 and 51%, respectively) and the fruits (19.2 and 12%, respectively). There were fewer edible underground organs in Marseille (4.8%) than in Acıgöl (10%). Proto-cereals including *Secale* sp. could also be consumed and represent an interesting carbohydrate resource for all omnivores, including hominins. They could also feed on *Castanea*, *Corylus* sp., *Juglans* sp., *Prunus* t., *Cornus sanguinea* sp., *Malus acerba*, *Vitis* sp., *Carduus* t., *Urtica* t., *Malva* sp. and many other plants listed in Supplementary File S7. Hardy [91] indicates that plant resources

could constitute the bulk of the diet, even in regions where biodiversity was reduced. To this could be added marine animal resources because the tufa of Marseille were close to the Mediterranean Sea in the Lower Pleistocene or those coming from terrestrial animal hunting. No archaeological research has been carried out in the Marseille calcareous tufa, and few results have been obtained apart from the discovery of the remains of *Mammuthus meridionalis* and *Palaeoloxodon antiquus*. In contemporaneous western Mediterranean sites, we observe that hominins had access to a wide choice of edible animals, from fish to snails and insects to reptiles [92] and from small to large mammals [74,93]. The potential plant and animal food resources were therefore very diversified, as were the ecosystems at that time, before the global cooling of the climate and the deleterious action of human populations.

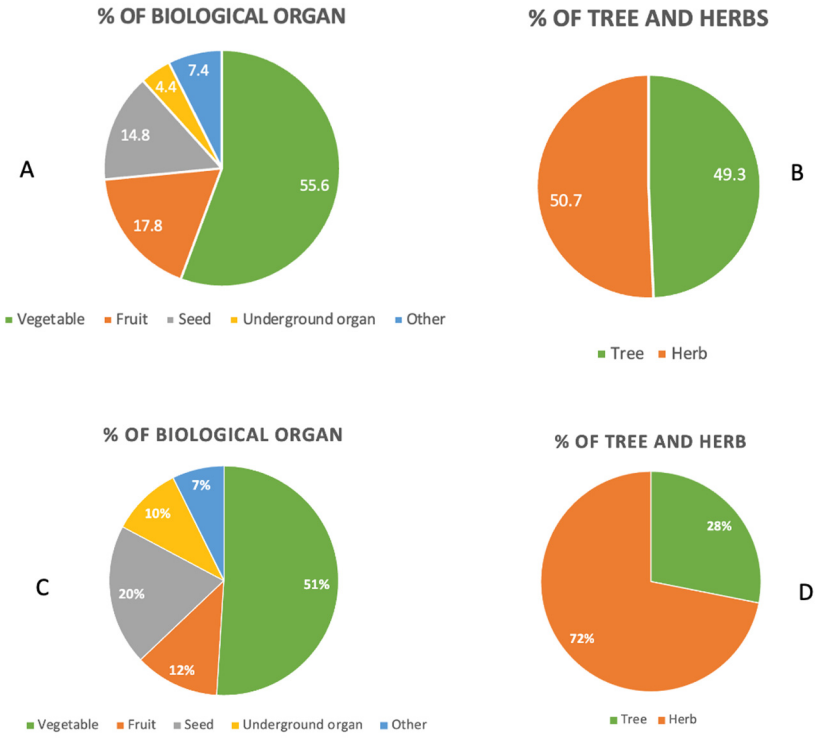

Figure 17. The potential plant diet reconstructed from pollen data from the Marseille tufa (**A**,**B**) and Acıgöl (**C**,**D**), Turkey (redrawn [5]).

The salt resource in the Marseille area should have been abundant near the seashore due to the seasonally dry and hot climate. Did hominins have potential access to salt-preserved meat resources? This is a question that we can put forward despite the lack of evidence. Another legitimate question is whether the animal protein they ate was cooked or not. To date, archaeological evidence of significant fire use in Europe dates back 300,000 to 400,000 years [94]; however, it is possible that hominins may have consumed meat (and even roots) accidentally cooked by natural fires [95]. The numerous micro-charcoals present in the samples studied show the existence of fires which affected essentially the trees (square shape of the micro-charcoals). Whatever the origin of these fires, natural or anthropogenic, man, who is an opportunistic animal, was thus able to consume cooked food and realise the benefits he could derive from it since cooking food promotes its digestibility. The oldest traces of fires were found in eastern Africa and dated to 1.5–1.6 Ma [94,96,97]. The discovery of micro-charcoals in the ancient natural (and non-archaeological) site that we study within the framework of the ANR FOOD-RE indicates the existence of fires, natural or not, in the lake series of SW Turkey, Acıgöl and Burdur for more than 3 Ma. This means that man knew about fires and perhaps the advantages he could derive from them in terms of hunting strategy or consuming digestible food.

5.5. A Cooler and Wetter Climate

The reconstructed climate at Marseille shows a cooler climate, mainly during winter, and wetter conditions compared to modern values (Figure 16). The reconstructed temperatures based on pollen data are in agreement with the very negative $\delta^{13}C$ values of the calcareous tufa, which is assumed to have formed in cool water.

Similar to today, the climate corresponds to a warm temperate climate with hot dry summers according to the Köppen–Geiger climate classification [98]. Pollen results sometimes show differences in vegetation records depending on the samples (Figure 13). Despite these differences, the reconstructed climate parameters from the various samples consistently indicate cooler and wetter conditions compared to modern values, except for sample 2. For sample 2 (La Viste 2021), the reconstructed climate values are closer to modern conditions for temperatures and precipitation, except for winter temperatures. This difference may be due to the presence of *Artemisia* up to 20%, whereas this taxon only represents 6% of the maximum signal in the other samples and the presence of *Olea* up to 6% (Figure 13). *Artemisia* is a steppe taxon and *Olea* a Mediterranean taxon that develop in warm and dry climatic conditions. In contrast to sample 2, sample 3 (Saint-Exupéry High School) does not show significant deviation despite a similar percentage for the steppic group (Figure 13). This could be related to the higher percentage of Poaceae, which is generally associated with cooler and wetter conditions compared to *Artemisia*.

The time period covered by our record extends from 1.2 to 0.9 Ma. This period includes the mid-Pleistocene transition (MPT), dated between 1.25 Ma and 0.75 Ma [99]. The MPT is marked by the transition from 41 kyr climatic cycles to 100 kyr cycles with longer and more intense glaciations. The 41 kyr cyclicity corresponded to the repeat time of the obliquity cycle, while the 100 kyr cyclicity is more complex and is related to the eccentricity (100 kyr), obliquity (41 kyr) and precession (23 kyr) cycles [100]. In terms of vegetation changes, the Early–Middle Pleistocene is characterised by a progressive decline in subtropical taxa and the diversification of Mediterranean vegetation [101]. The pollen data recorded at Marseille illustrate this trend with the absence of subtropical taxa and the presence of Mediterranean taxa, such as *Olea* and *Quercus ilex*.

In the Mediterranean region, climate reconstructions based on pollen from the Alboran Sea (ODP 976) and Italy show cooler conditions compared to modern values during the MPT, similar to the Marseille samples [49,101]. The ODP 976 sequence records colder conditions for winter temperatures during glacial and interglacial periods between 1.09 and 0.9 Ma [49]. For annual temperature, the ODP 976 sequence generally shows colder temperatures except for some interglacial periods where the temperatures are close to or higher than modern values [49]. In Italy, the climate records indicate colder temperatures in winter during glacial and interglacial periods between 1.4 and 0.9 Ma [101]. Regarding precipitation, the climate reconstructions from the Alboran Sea (ODP 976) show wetter or similar conditions compared to modern values during interglacial periods and drier conditions during glacial periods between 1.09 and 0.9 Ma [49]. In contrast, the precipitation reconstructions from Italy indicate generally similar or drier conditions compared to modern values during interglacial periods and similar conditions during glacial periods between 1.4 and 0.9 Ma [101]. The climate reconstructions from Marseille show slightly colder conditions (except for sample 2), making it difficult to assign samples to a glacial or interglacial period, especially as it is known that in the Mediterranean region ancient glacial phases are less pronounced than more recent glacial phases [101]. However, the climate results from Marseille show wetter conditions than the modern ones, suggesting that the samples are more closely related to the Alboran Sea climatic type [49] and correspond to an interglacial period. Concerning sample 2, which is characterised by temperatures close to modern values and thus warmer compared to the other Marseille samples, this suggests that the sample is associated with an interglacial period characterised by precipitation levels similar to modern values. Therefore, the Marseille samples originate from interglacial periods, and the climate of this region is more similar to that observed in the Alboran Sea [48] rather than in Italy [101].

6. Conclusions

The study of the tufa of Marseille is enabling us to improve our knowledge of the palaeoenvironments of the Early Pleistocene on the northwestern edge of the Mediterranean. Previous studies date back to the end of the 19th century and the beginning of the 20th century. Our multiproxy study shows that these tufa were formed ca. 1 Ma ago (Jaramillo subchron) in a diversified depositional environment and cold water. The vegetation consisted of a mosaic of Mediterranean vegetation dominated by oak forest and pine forest. Ecosystems and taxa that are now absent from the Marseille basin were identified, such as the chestnut grove that could grow on the Oligocene clays, *Juglans* and *Platanus* that were present in the riverine forest and *Picea*, *Fagus* and *Abies*, trees whose pollen is not widely dispersed by wind and which were at low altitude. The potential vegetal diet available to animals, including hominins, was diversified and included 60% of the vegetative part of plants and 19% of fruit. The record of proto-cereal pollen is unusual and shows that these plants, rich in carbohydrates, were able to contribute to the potential diet. The nitrophilous plants and spores of coprophilous fungi found in the pollen assemblages could indicate that large herbivores were present in the Marseille basin. It is possible that, as in Anatolia, grazing, trampling and the input of nitrogen modified the genome of wild Poaceae, leading to the appearance of cereals. Along with the Acıgöl series in southwestern Anatolia, the Marseille basin is a site where cereals were able to develop in open environments frequented by herbivores attracted by the presence of fresh water. Globally, the climate was a little cooler and wetter than it is today. Overall, we claim that, besides the lack of evidence for hominins presence, the Marseille basin was an ideal habitat for hominins when they arrived there about 1 Ma ago.

Supplementary Materials: The following supporting information can be downloaded at https://www.mdpi.com/article/10.3390/geosciences14080211/s1, Supplementary File S1: List and location of pollen samples from the Marseille tufa, Supplementary File S2: Row counting of the Marseille tufa samples, Supplementary File S3: Statistical parameters of the modern analogue technique (MAT), weighted averaging partial least squares regression (WA-PLS), boosted regression trees (BRT), random forest (RF) and climatic amplitude method (CAM) methods applied on the European and Mediterranean pollen dataset, Supplementary File S4 sheet 1: Palaeomagnetic results table of La Viste section (TRM), Supplementary File S4 sheet 2 [102]: Palaeomagnetic results table for Saint Exupéry (SX), Carrefour Market (CAM) and Calade (CAL) sections, Supplementary File S5. Carbon and oxygen isotope composition of bulk carbonates: lower Pleistocene calcareous tufas from the Marseille Basin, Supplementary File S6. Ecological classification of pollen taxa used to draw pollen diagrams, Supplementary File S7. List of edible plants from the Marseille tufa.

Author Contributions: Archaeology: P.M.; climate reconstruction: M.R., S.F. and O.P.; magnetism: P.R., F.D. and S.B.D.C.; sedimentology: F.F.; palynology: V.A., B.G. and E.C. All authors have read and agreed to the published version of the manuscript.

Funding: This work received financial funding from ANR FOOD-RE (ANR-21-CE03-0019) V. Andrieu leader 1 April 2022 (https://www.cerege.fr/fr/sciences/terre-et-planetes/projets-terre-et-planete/anr-food-re/).

Data Availability Statement: All data generated or analysed during this study are included in this published article.

Acknowledgments: We would particularly like to thank IMERA (Institute for Advanced Studies of Aix-Marseille University) and the Micropaleontological Preparation Laboratory (CEREGE).

Conflicts of Interest: The authors declare no conflicts of interest.

References

1. Asmerom, Y.; Polyak, V.J.; Wagner, J.D.M.; Patchett, P.J. Hominin expansion into Central Asia during the last interglacial. *Earth Planet. Sci. Lett.* **2018**, *494*, 148–152. [CrossRef]
2. Barboni, B.; Ashley, G.; Bourel, B.; Arraiz, H.; Mazur, J.C. Springs, Palm groves, and the record of early hominins in Africa. *Rev. Palaeobot. Palynol.* **2019**, *266*, 23–41. [CrossRef]

3. Lebatard, A.E.; Alcicek, M.C.; Rochette, P.; Khatib, S.; Vialet, A.; Boulbes, N.; Bourlès, D.L.; Demory, F.; Guipert, G.; Mayda, S.; et al. Dating the Homo erectus bearing travertine from Kocabaş (Denizli, Turkey) at least 1.1 Ma. *Earth Planet. Sci. Lett.* **2014**, *390*, 8–18. [CrossRef]
4. Rausch, L.; Alçiçek, H.; Vialet, A.; Boulbes, N.; Mayda, S.; Titov, V.V.; Stoica, M.; Charbonnier, S.; Abels, H.A.; Tesakov, A.S.; et al. An integrated reconstruction of the Early Pleistocene palaeoenvironment of Homo erectus in the Denizli Basin (SW Turkey). *Geobios* **2019**, *57*, 77–95. [CrossRef]
5. Andrieu-Ponel, V.; Rochette, P.; Demory, F.; Alcicek, H.; Boulbes, N.; Bourlès, N.; Helvaci, C.; Lebatard, A.; Mayda, S.; Moigne, A.M.; et al. Continuous presence of proto-cereals in Anatolia since 2.3 Ma, and their possible co-evolution with large herbivores and hominins. *Sci. Rep. (Nat.)* **2021**, *11*, 8914. [CrossRef] [PubMed]
6. Dupire, S. Etude Cartographique à 1/ 25.000 de la Zone Sud du Basin de Marseille. Les Travertins de Marseille: Aperçu Géomorphologique et Néotectonique. Ph.D. Thesis, Université de Provence, Marseille, France, 1985; p. 105.
7. Toro Moyano, I.; Martinez Navarro, B.; Agusti, J.; Souday, C.; Bermudez de Castro, J.M.; Martinon Torres, M.; Fajardo, B.; Duval, M.; Falgueres, C.; Oms, O.; et al. The oldest human fossil in Europe, from Orce (Spain). *J. Hum. Evol.* **2013**, *65*, 1–9. [CrossRef]
8. Alvarez, C.; Pares, J.M.; Granger, D.; Duval, M.; Sala, R.; Toro, I. New magnetostratigraphic and numerical age of the Fuente Nueva-3 site (Guadix-Baza basin, Spain). *Quat. Int.* **2015**, *389*, 224–234. [CrossRef]
9. Carbonell, E.; Bermudez de Castro, J.M.; Pares, J.M.; Perez Gonzalez, A.; Cuenca Bescos, G.; Olle, A.; Mosquera, M.; Huguet, R.; van der Made, J.; Rosas, A.; et al. The first hominin of Europe. *Nature* **2008**, *452*, 465–469. [CrossRef] [PubMed]
10. Huguet, R.; Vallverdú, J.; Rodríguez Álvarez, X.P.; Terradillos Bernal, M.; Bargalló, A.; Lombera Hermida, A.; Menéndez, L.; Modesto Mata, M.; Van der Made, J.; Soto, M.; et al. Level TE9c of Sima del Elefante (Sierra de Atapuerca, Spain): A comprehensive approach. *Quat. Int.* **2017**, *433*, 278–295. [CrossRef]
11. Michel, V.; Shen, C.C.; Woodhead, J.; Hu, H.M.; Wu, C.C.; Moullé, P.E.; Khatib, S.; Cauche, D.; Moncel, M.H.; Valensi, P.; et al. New dating evidence of the early presence of hominins in Southern Europe. *Sci. Rep. (Nat.)* **2017**, *7*, 10074. [CrossRef]
12. Bourguignon, L.; Crochet, J.Y.; Capdevila, R.; Ivorra, J.; Antoine, P.O.; Agustí, J.; Barsky, D.; Blain, H.A.; Boulbes, N.; Bruxelles, L.; et al. Bois-de-Riquet (Lézignan-la-Cèbe, Hérault): A late Early Pleistocene archaeological occurrence in southern France. *Quat. Int.* **2016**, *393*, 24–40. [CrossRef]
13. de Saporta, G. Sur la flore des tufs quaternaires en Provence. In *Extrait des Comptes-Rendus de la 33ème Session du Congrès Scientifique de France*; Typographie Remontet-Aubin: Aix-en-Provence, France, 1867; pp. 3–32.
14. Pons, A. Les macroflores quaternaires de France. In *Etudes Françaises sur le Quaternaire*; VIIIth INQUA Congress: Paris, France, 1969; pp. 85–93.
15. Médail, F. Mise en place de la flore: Approche biogéographique. In *La Flore Remarquable des Bouches-du-Rhône*; Pirès, M., Pavon, D., Eds.; Plantes, milieux naturels, paysages; Biotope: Mèze, France, 2018; pp. 22–50.
16. Bonifay, E. La tectonique récente du bassin de Marseille dans le cadre de l'évolution post-Miocène du littoral méditerranéen français. *Bull. Soc. Gél. France* **1967**, *IX*, 549–560.
17. Villeneuve, M. (Ed.) *Mémoire Explicatif*, 3rd ed.; Carte géol. France (1/50,000), feuille Aubagne-Marseille; BRGM: Orléans, France, 2018; 333p.
18. Bertini, A.; Minissale, A.; Ricci, M. Palynological approach in upper Quaternary terrestrial carbonates of central Italy: Anything but a 'mission impossible'. *Sedimentology* **2014**, *61*, 200–220. [CrossRef]
19. Ali, A.A.; Terral, J.F.; Girard, V.; Roiron, P. Les travertins à empreintes, témoins de la paléobiodiversité végétale. *Quaternaire* **2014**, *25*, 157–161. [CrossRef]
20. Kahlke, R.D.; García, N.; Kostopoulos, D.S.; Lacombat, F.; Lister, A.M.; Mazza, P.; Titov, V.V. Western Palaearctic palaeoenvironmental conditions during the Early and early Middle Pleistocene inferred from large mammal communities, and implications for hominin dispersal in Europe. *Quat. Sci. Rev.* **2011**, *30*, 1368–1395. [CrossRef]
21. Rousselière, F. Les Proboscidiens du basin de Marseille. *Bull. Du Musée Anthropol. Et De Préhistoire De Monaco* **2004**, *44*, 39–48.
22. Muttoni, G.; Scardia, G.; Kent, D.V. Early hominins in Europe: The Galerian migration hypothesis. *Quat. Sci. Rev.* **2018**, *180*, 1–29. [CrossRef]
23. Laurent, L. Appendice: Paléobotanique. In *Les Bouches-du-Rhône*; Encyclopédie départementale. Honoré Champion, Marseille; Archives Départementales des Bouches-du-Rhône: Paris, France; Marseille, France, 1932; pp. 339–391.
24. Dubar, M.; Magnin, F. Présence d'hélicelles (Helicellinae) dans le Pliocène du Midi de la France, nouvelles données sur la dispersion du groupe au Pléistocène inférieur, implications paléoclimatiques. *GÉObios* **1992**, *25*, 357–366. [CrossRef]
25. Triat-Laval, H. *Contribution Pollenanalytique et L'histoire Tardi- et Post-Glaciaire de la Végétation de la Basse Vallée du Rhône*; Thèse Université de Marseille: Marseille, France, 1978.
26. Lurcock, P.C.; Wilson, G.S. PuffinPlot: A versatile, user-friendly program for paleomagnetic analysis. *Geochem. Geophys. Geosystems* **2012**, *13*, Q06Z45. [CrossRef]
27. Channell, J.E.T.; Singer, B.S.; Jicha, B.R. Timing of Quaternary geomagnetic reversals and excursions in volcanic and sedimentary archives. *Quat. Sci. Rev.* **2020**, *228*, 1–29. [CrossRef]
28. Arenas-Abad, C.; Vázquez-Urbez, M.; Pardo-Tirapu, G.; Sancho-Marcén, C. Fluvial and associated carbonate deposits. In *Carbonates in Continental Settings: Facies, Environments and Processes, Developments in Sedimentology*; Alonso-Zarza, A.M., Tanner, L.H., Eds.; Elsevier: Amsterdam, The Netherlands, 2010; Volume 61, pp. 133–175.

29. Fournier, F.; Ouass, A.; Rochette, P.; Bromblet, P.; Léonide, P.; Conesa, G.; Marié, L.; Boularand, S.; D'Ovidio, A.-M.; Vigie, B.; et al. Provenance of sculptural limestones in protohistoric Provence (SE France): Insights from carbonate rock petrography and stable isotope geochemistry. *J. Archaeol. Sci. Rep.* **2023**, *48*, 103922. [CrossRef]
30. Nakagawa, T.; Brugiapaglia, E.; Digerfeldt, G.G.; Reille, M.; de Beaulieu, J.L.; Yasuda, Y. Dense-media separation as a more efficient pollen extraction method for use with organic sediment/deposit samples: Comparison with the conventional method. *Boreas* **1998**, *27*, 15–24. [CrossRef]
31. Reille, M. *Pollen et Spores d'Europe et d'Afrique du Nord*; Laboratoire de Botanique Historique et de Palynologie: Marseille, France, 1992.
32. Reille, M. *Pollen et Spores d'Europe et d'Afrique du Nord*; Supplement 1; Laboratoire de Botanique Historique et de Palynologie: Marseille, France, 1995.
33. Reille, M. *Pollen et Spores d'Europe et d'Afrique du Nord*; Supplement 2; Laboratoire de Botanique Historique et de Palynologie: Marseille, France, 1998.
34. Beug, H.J. *Leitfaden der Pollenbestimmung für Mitteleuropa und Angrenzende Gebiete*; Dr. Friedrich Pfeil: Munich, Germany, 2004.
35. Cugny, C.; Mazier, F.; Galop, D. Modern and fossil non-pollen palynomorphs from the Basque mountains (western Pyrenees, France): The use of coprophilous fungi to reconstruct pastoral activity. *Veg. Hist. Archaeobot.* **2010**, *19*, 391–408. [CrossRef]
36. Haas, J.N. Fresh insights into the palaeoecological and palaeoclimatological value of Quaternary non-pollen palynomorphs. *Veget. Hist. Archaeobot.* **2010**, *19*, 389–560. [CrossRef]
37. Van Geel, B.; Aptroot, A. Fossil ascomycetes in Quaternary deposits. *Nova Hedwig.* **2006**, *82*, 313–329. [CrossRef]
38. Brewer, S.; Guiot, J.; Sánchez-Goñi, M.F.; Klotz, S. The Climate in Europe during the Eemian: A Multi-Method Approach Using Pollen Data. *Quat. Sci. Rev.* **2008**, *27*, 2303–2315. [CrossRef]
39. Peyron, O.; Magny, M.; Goring, S.; Joannin, S.; de Beaulieu, J.-L.; Brugiapaglia, E.; Sadori, L.; Garfi, G.; Kouli, K.; Ioakim, C.; et al. Contrasting Patterns of Climatic Changes during the Holocene across the Italian Peninsula Reconstructed from Pollen Data. *Clim. Past* **2013**, *9*, 1233–1252. [CrossRef]
40. Salonen, J.S.; Korpela, M.; Williams, J.W.; Luoto, M. Machine-Learning Based Reconstructions of Primary and Secondary Climate Variables from North American and European Fossil Pollen Data. *Sci. Rep.* **2019**, *9*, 15805. [CrossRef] [PubMed]
41. Guiot, J. Methodology of the Last Climatic Cycle Reconstruction in France from Pollen Data. *Palaeogeogr. Palaeoclimatol. Palaeoecol.* **1990**, *80*, 49–69. [CrossRef]
42. ter Braak, C.J.F.; Juggins, S. Weighted Averaging Partial Least Squares Regression (WA-PLS): An Improved Method for Reconstructing Environmental Variables from Species Assemblages. *Hydrologia* **1993**, *269*, 485–502. [CrossRef]
43. De'ath, G. Boosted Trees for Ecological Modeling and Prediction. *Ecology* **2007**, *88*, 243–251. [CrossRef]
44. Elith, J.; Leathwick, J.R.; Hastie, T. A Working Guide to Boosted Regression Trees. *J. Anim. Ecol.* **2008**, *77*, 802–813. [CrossRef] [PubMed]
45. Breiman, L. Random Forests. *Mach. Learn.* **2001**, *45*, 5–32. [CrossRef]
46. Prasad, A.M.; Iverson, L.R.; Liaw, A. Newer Classification and Regression Tree Techniques: Bagging and Random Forests for Ecological Prediction. *Ecosystems* **2006**, *9*, 181–199. [CrossRef]
47. Fauquette, S.; Guiot, J.; Suc, J.-P. A Method for Climatic Reconstruction of the Mediterranean Pliocene Using Pollen Data. *Palaeogeogr. Palaeoclimatol. Palaeoecol.* **1998**, *144*, 183–201. [CrossRef]
48. Davis, B.A.S.; Brewer, S.; Stevenson, A.C.; Guiot, J. The Temperature of Europe during the Holocene Reconstructed from Pollen Data. *Quat. Sci. Rev.* **2003**, *22*, 1701–1716. [CrossRef]
49. Joannin, S.; Bassinot, F.; Nebout, N.C.; Peyron, O.; Beaudouin, C. Vegetation Response to Obliquity and Precession Forcing during the Mid-Pleistocene Transition in Western Mediterranean Region (ODP Site 976). *Quat. Sci. Rev.* **2011**, *30*, 280–297. [CrossRef]
50. Salonen, J.S.; Luoto, M.; Alenius, T.; Heikkilä, M.; Seppä, H.; Telford, R.J.; Birks, H.J.B. Reconstructing Palaeoclimatic Variables from Fossil Pollen Using Boosted Regression Trees: Comparison and Synthesis with Other Quantitative Reconstruction Methods. *Quat. Sci. Rev.* **2014**, *88*, 69–81. [CrossRef]
51. Sinopoli, G. Vegetation and Climate Reconstruction during the Last Interglacial Complex: The Pollen Record of Lake Ohrid (Albania/Fyrom), the Oldest European Lake. Ph.D. Thesis, Università di Roma, University of Montpellier, Rome, Italy, 2017.
52. Juggins, S. *R Package*, Version 0.9-26; Analysis of Quaternary Science Data. 2020.
53. Robles, M.; Peyron, O.; Brugiapaglia, E.; Ménot, G.; Dugerdil, L.; Ollivier, V.; Ansanay-Alex, S.; Develle, A.-L.; Tozalakyan, P.; Meliksetian, K.; et al. Impact of Climate Changes on Vegetation and Human Societies during the Holocene in the South Caucasus (Vanevan, Armenia): A Multiproxy Approach Including Pollen, NPPs and brGDGTs. *Quat. Sci. Rev.* **2022**, *277*, 107297. [CrossRef]
54. Chevalier, M.; Davis, B.A.S.; Heiri, O.; Seppä, H.; Chase, B.M.; Gajewski, K.; Lacourse, T.; Telford, R.J.; Finsinger, W.; Guiot, J.; et al. Pollen-Based Climate Reconstruction Techniques for Late Quaternary Studies. *Earth-Sci. Rev.* **2020**, *210*, 103384. [CrossRef]
55. Liaw, A.; Wiener, M. Classification and Regression by randomForest. *R News* **2002**, *2*, 18–22.
56. Hijmans, R.J.; Phillips, S.; Leathwick, J.; Elith, J. *R Package*, version 1.3-5; Dismo: Species Distribution Modeling. 2021.
57. Dugerdil, L.; Joannin, S.; Peyron, O.; Jouffroy-Bapicot, I.; Vannière, B.; Boldgiv, B.; Unkelbach, J.; Behling, H.; Ménot, G. Climate Reconstructions Based on GDGT and Pollen Surface Datasets from Mongolia and Baikal Area: Calibrations and Applicability to Extremely Cold–Dry Environments over the Late Holocene. *Clim. Past* **2021**, *17*, 1199–1226. [CrossRef]
58. Vázquez Urbez, M.; Arenas, C.; Pardo, G. A sedimentary facies model for stepped, fluvial tufa systems in the Iberian Range (Spain): The Quaternary Piedra and Mesa valleys. *Sedimentology* **2012**, *59*, 502–526. [CrossRef]

59. Fick, S.E.; Hijmans, R.J. WorldClim 2: New 1-km Spatial Resolution Climate Surfaces for Global Land Areas. *Int. J. Climatol.* **2017**, *37*, 4302–4315. [CrossRef]
60. Pentecost, A. *Travertine*; Springer: Berlin/Heidelberg, Germany, 2005; 445p.
61. Gandin, A.; Capezzuoli, E. Travertine versus calcareous tufa: Distinctive pterographic features and stable isotope signatures. *Ital. J. Quat. Sci.* **2008**, *21*, 125–136.
62. Andrews, J.E.; Pedly, M.; Dennis, P.F. Palaeoenvironmental records in Holocene Spanish tufas: A stable isotope approach in search of reliable climatic archives. *Sedimentology* **2000**, *47*, 961–978. [CrossRef]
63. Arenas, C.; Guttiérrez, F.; Osacar, C.; Sancho, C. *Sedimentology* and geochemistry of fluvio-lacustrine tufa deposits controlled by evaporite solution subsidence in the Central Ebro Depression, NE Spain. *Sedimentology* **2000**, *47*, 883–909. [CrossRef]
64. Cronquist, A. *An Integrated System of Classification of Flowering Plants*; Columbia University Press: New York, NY, USA, 1981; p. 1262.
65. Djamali, M.; Cilleros, K. Statistically significant minimum pollen count in Quaternary pollen analysis; the case of pollen-rich lake sediments. *Rev. Palaeobot. Palynol.* **2020**, *275*, 104156. [CrossRef]
66. Juggins, S. 2014. Available online: https://www.staff.ncl.ac.uk/stephen.juggins/software/C2Home.htm (accessed on 16 April 2014).
67. Altolaguirre, Y.; Bruch, A.A.; Gibert, L. A long Early Pleistocene pollen record from Baza Basin (SE Spain): Major contributions to the palaeoclimate and palaeovegetation of Southern Europe. *Quat. Sci. Rev.* **2020**, *231*, 106199. [CrossRef]
68. Ponel, P.; Andrieu-Ponel, V.; Djamali, M.; Lahijani, H.; Leydet, M.; Mashkour, M. Fossil beetles as possible evidence for transhumance during the middle and late Holocene in the high mountains of Talysch (Talesh) in NW Iran? *Environ. Archaeol.* **2013**, *18*, 201–210. [CrossRef]
69. Vernet, J.L. History of the Pinus sylvestris and *Pinus nigra* ssp. salzmannii forest in the Sub-Mediterranean mountains (Grands Causses, Saint-Guilhem-le-Désert, southern Massif Central, France) based on charcoal from limestone and dolomitic deposits. *Veg. Hist. Archaeobotany* **2006**, *16*, 23–42. [CrossRef]
70. INPN. Pin de salzmann (fiche I.N.P.N.: Inventaire National du Patrimoine Naturel). Available online: https://inpn.mnhn.fr/espece/cd_nom/138844 (accessed on 29 May 2024).
71. Roiron, P.; Chabal, L.; Figueiral, I.; Terral, J.F.; Adam, A.A. Palaeobiogeography of Pinus nigra Arn. subsp. salzmannii (Dunal) Franco in the north-western Mediterranean Basin: A review based on macroremains. *Rev. Palaeobot. Palynol.* **2013**, *194*, 1–11. [CrossRef]
72. Molinier, R. *Catalogue des Plantes Vasculaires des Bouches-du-Rhône*; Muséum d'Histoire Naturelle de Marseille: Marseille, France, 1981; 375p.
73. Joannin, S.; Ciaranfi, N.; Stefanelli, S. Vegetation changes during the late Early Pleistocene at Montalbano Jonico (Province of Matera, southern Italy) based on pollen analysis. *Palaeogeogr. Palaeoclimatol. Palaeoecol.* **2008**, *270*, 92–101. [CrossRef]
74. Magri, D.; Di Rita, F.; Palombo, M.R. An Early Pleistocene interglacial record from an intermontane basin of central Italy (Scoppito, L'Aquila). *Quat. Int.* **2010**, *225*, 106–113. [CrossRef]
75. Russo-Ermolli, E.; Aucelli, P.P.C.; Di Rollo, A.; Mattei, A.; Petrosino, P.; Porreca, M.; Rosskopf, C. An intergrated stratigraphical approach to the late Middle Pleistocene succession of the Sessano lacustrine basin (Molise, Italy). *Quat. Int.* **2010**, *225*, 114–127. [CrossRef]
76. Orain, R.; Lebreton, V.; Russo-Ermolli, E.; Semah, A.M.; Nomade, S.; Shao, Q.; Bahain, J.J.; Thun Hohenstein, U.; Peretto, C. Hominin responses to environmental changes during the Middle Pleistocene in central and southern Italy. *Clim. Past* **2013**, *9*, 687–697. [CrossRef]
77. Suc, J.-P.; Popescu, S.-M.; Fauquette, S.; Bessedik, M.; Jiménez-Moreno, G.; Bachiri-Taoufiq, N.; Zheng, Z.; Médail, F.; Klotz, S. Reconstruction of Mediterranean flora, vegetation and climate for the last 23 million years based on an extensive pollen dataset. *Ecol. Mediterr.* **2018**, *44*, 53–86. [CrossRef]
78. Magri, D.; Palombo, M.R. Early to middle pleistocene dynamics of plant and mammal communities in south west Europe. *Quat. Int.* **2013**, *288*, 63–72. [CrossRef]
79. Romey, C.; Vella, C.; Rochette, P.; Andrieu-Ponel, V.; Magnin, F.; Veron, A.; Landuré, C.; Anne-D'Ovidio, A.M.; Delanghe-Sabatier, D. Environmental imprints of landscape evolution and human activities during the Holocene in a small catchment of the Calanques Massif (Cassis, southern France). *Holocene* **2015**, *25*, 1454–1469. [CrossRef]
80. Caudullo, G.; Tinner, W. *Abies*-Circum-Mediterranean firs in Europe: Distribution, habitat, usage and threats. In *European Atlas of Forest Tree Species*; San-Miguel-Ayanz, J., de Rigo, D., Caudullo, G., Houston Durrant, T., Mauri, A., Eds.; Publications Office of the EU: Luxembourg, 2016; p. e015be7+.
81. Garcia Anton, M.; Sainz Ollero, H. Pollen records from the middle Pleistocene Atapuerca site (Burgos, Spain). *Palaeogeogr. Palaeoclimatol. Palaeoecol.* **1991**, *85*, 199–206. [CrossRef]
82. Postigo Mijarra, J.M.; Burjachs, F.; Gomez Manzaneque, F.; Morla, C. A palaeoecological interpretation of the lower-middle Pleistocene Cal Guardiola site (Terrassa, Barcelona, NE Spain) from the comparative study of wood and pollen samples. *Rev. Palaeobot. Palynol.* **2007**, *146*, 247–264. [CrossRef]
83. Leroy, S.; Ambert, P.; Suc, J.P. Pollen record of the Saint-Macaire maar (Hérault, S. France): A lower Pleistocene glacial phase in the Languedoc coastal plain. *Rev. Palaeobot. Palynol.* **1994**, *80*, 149–157. [CrossRef]
84. Girard, M. Résultats préliminaire de l'analyse pollinique. In L'épave romaine de La Madrague de Giens (Var). *Gallia* **1978**, *XXXIV*, 112–116.

85. Andrieu-Ponel, V.; Ponel, P.; Jull, A.J.T.; de Beaulieu, J.L.; Bruneton, H.; Leveau, P. Towards the reconstruction of the Holocene vegetation history of Lower Provence: Two new pollen profiles from Marais des Baux. *Veg. Hist. Archaeobotany* **2000**, *9*, 71–85. [CrossRef]
86. Andrieu-Ponel, V.; Ponel, P.; Bruneton, H.; Leveau, P. Palaeoenvironments and cultural landscape of the last 2000 years reconstructed from pollen and coleopteran records in the lower Rhône valley, southern France. *Holocene* **2000**, *10*, 341–355. [CrossRef]
87. Groman-Yaroslavski, I.; Weiss, E.; Nadel, D. Composite sickles and cereal harvesting methods at 23,000-years-Old Ohalo II, Israel. *PLoS ONE* **2016**, *11*, e0167151. [CrossRef] [PubMed]
88. Bonnier, G.; Douin, R. *Flore Complète Illustrée en Couleurs de France, Suisse et Belgique*; Re-édition modern; Belin, Germany; Paris, France, 1990.
89. Couplan, F. La cuisine sauvage. Comment accommoder mille plantes oubliées. In *Encyclopédie des Plantes Comestibles de l'Europe*; Equilibres: Condé-sur-Noireau, France, 1989; Volume 2, 512p.
90. de Cortes Sanchez-Mata, M.; Tardio, J. *Mediterranean Wild Edible Plants Ethnobotany and Food Composition Tables*; Springer: Berlin/Heidelberg, Germany, 2016.
91. Hardy, K. Plant use in the Lower and Middle Palaeolithic: Food, medicine and raw materials. *Quat. Sci. Rev.* **2018**, *191*, 393–405. [CrossRef]
92. Rodríguez, J.; Burjachs, F.; Cuenca Bescós, G.; García, N.; Van der Made, J.; Pérez González, A.; Blain, H.A.; Expósito, I.; López García, J.M.; García Antón, M.; et al. One million years of cultural evolution in a stable environment at Atapuerca (Burgos, Spain). *Quat. Sci. Rev.* **2011**, *30*, 1396–1412. [CrossRef]
93. Pelletier, M.; Cochard, D.; Boudadi-Maligne, M.; Crochet, J.Y.; Bourguignon, L. Lower Pleistocene leporids (Lagomorpha, Mammalia) in Western Europe: New data from the Bois-de-Riquet (Lézignan-la-Cèbe, Hérault, France). *Comptes Rendus Palevol* **2015**, *14*, 371–385. [CrossRef]
94. Roebroeks, W.; Villa, P. On the earliest evidence for habitual use of fire in Europe. *Proc. Natl. Acad. Sci. USA* **2011**, *108*, 5209–5214. [CrossRef]
95. Gowlett, J.A.J. The discovery of fire by humans: A long and convoluted process. *Philos. Trans. R. Soc. B* **2016**, *371*, 20150164. [CrossRef]
96. Bellomo, R.V.; Kean, W.F. Evidence of hominid controlled fire at the FxJj20 site complex, Karari escarpment. Appendix 4A. In *Koobi Fora Research Project Volume 5: Plio-Pleistocene Archaeology*; Isaac, G.L., Isaac, B., Eds.; Clarendon Press: Oxford, UK, 1997; pp. 224–233.
97. Rowlett, R.M. Fire control by Homo erectus in East Africa and Asia. *Acta Anthropol. Sin.* **2000**, *19*, 198–208.
98. Kottek, M.; Grieser, J.; Beck, C.; Rudolf, B.; Rubel, F. World Map of the Köppen-Geiger Climate Classification Updated. *Meteorol. Z.* **2006**, *15*, 259–263. [CrossRef] [PubMed]
99. Herbert, T.D. The Mid-Pleistocene Climate Transition. *Annu. Rev. Earth Planet. Sci.* **2023**, *51*, 389–418. [CrossRef]
100. Hays, J.D.; Imbrie, J.; Shackleton, N.J. Variations in the Earth's Orbit: Pacemaker of the Ice Ages. *Science* **1976**, *194*, 1121–1132. [CrossRef] [PubMed]
101. Combourieu-Nebout, N.; Bertini, A.; Russo-Ermolli, E.; Peyron, O.; Klotz, S.; Montade, V.; Fauquette, S.; Allen, J.; Fusco, F.; Goring, S.; et al. Climate Changes in the Central Mediterranean and Italian Vegetation Dynamics since the Pliocene. *Rev. Palaeobot. Palynol.* **2015**, *218*, 127–147. [CrossRef]
102. Kirschvink, J.L. The least-squares line and plane and the analysis of palaeomagnetic data. *Geophys. J. Int.* **1980**, *62*, 699–718. [CrossRef]

Disclaimer/Publisher's Note: The statements, opinions and data contained in all publications are solely those of the individual author(s) and contributor(s) and not of MDPI and/or the editor(s). MDPI and/or the editor(s) disclaim responsibility for any injury to people or property resulting from any ideas, methods, instructions or products referred to in the content.